INSTITUT D'AERONOMIE SPATIALE DE BELGIQUE

3 - Avenue Circulaire
B - 1180 BRUXELLES

AERONOMICA ACTA

A - N° 229 - 1981

Effects of solar variations on the upper atmosphere

by

G. KOCKARTS

BELGISCH INSTITUUT VOOR RUIMTE-AERONOMIE

3 - Ringlaan
B - 1180 BRUSSEL

VOORWOORD

The paper "Effects of solar variations on the upper atmosphere" has been presented at the 14th ESLAB Symposium in Scheveningen (16-19 September 1980). It will be published in Solar Physics, 1981.

AVANT-PROPOS

L'Article "Effects of solar variations on the upper atmosphere" a été présenté au cours du 14ème Symposium ESLAB à Scheveningen (16-19 september 1980). Il sera publié dans Solar Physics, 1981.

VOORWOORD

De tekst "Effects of solar variations on the upper atmosphere" werd voorgedragen op het 14de ESLAB Symposium die plaatsvond in Scheveningen (16 - 19 september 1980). Deze tekst zal in Solar Physics 1981 verschijnen.

VORWORT

Die Arbeit "Effects of solar variations on the upper atmosphere" wurde zum 14. ESLAB Symposium in Scheveningen (16.-19. September 1980) vorgestellt. Sie wird in Solar Physics 1981 herausgegeben werden.

EFFECTS OF SOLAR VARIATIONS ON THE UPPER ATMOSPHERE

by

G. KOCKARTS

Institut d'Aéronomie Spatiale
3 Avenue Circulaire
B-1180 Bruxelles, Belgium

Abstract

Several semi-empirical models of the terrestrial upper atmosphere are presently available. These models take into account solar activity effects by using the solar decimetric flux as an index. Such a procedure is a consequence of the lack of continuous determinations of the solar spectrum directly responsible for the physical structure of the upper atmosphere. Variations of the thermopause temperature are discussed. Using five sets of solar irradiances measured in the ultraviolet and in the extreme ultraviolet, the penetration of solar radiation is analyzed as a function of solar activity. Several examples of absorption profiles and ion production rates are discussed for variable conditions. Various energetic effects are also described. All computations are made for physical conditions above Scheveningen (52.08°N) where the 14th ESLAB symposium was held.

Résumé

Il existe actuellement plusieurs modèles semi-empiriques de l'atmosphère supérieure de la terre. Ces modèles tiennent compte des effets de l'activité solaire en utilisant le flux solaire décimétrique comme index. Cette procédure est une conséquence de l'absence de détermination continue du spectre solaire directement responsable de la structure physique de l'atmosphère supérieure. Les variations de la température à la thermopause sont discutées. La pénétration du rayonnement solaire est analysée en fonction de l'activité solaire en utilisant cinq séries de flux solaires mesurés dans l'ultraviolet et dans l'extrême ultraviolet. Plusieurs exemples de profils d'absorption et de taux de productions ioniques sont discutés pour des conditions variables. Divers effets énergétiques sont discutés. Tous les calculs correspondent à des conditions physiques au-dessus de Scheveningen (52.08°N) où eut lieu le 14ème symposium ESLAB.

Samenvatting

Verschillende semi-empirische modellen van de aardse hogere atmosfeer zijn voor het ogenblik beschikbaar. Deze modellen houden rekening met zonne-activiteitseffecten door gebruik te maken van de decimetrische zonneflux als index. Een dergelijke methode is het gevolg van een gebrek aan continue bepalingen van het zonnespectrum dat rechtstreeks verantwoordelijk is voor de fysische structuur van de hogere atmosfeer. Veranderingen in de temperatuur van de thermopauze worden besproken. De penetratie van de zonnestraling in functie van de zonne-activiteit werd geanalyseerd door te steunen op vijf reeksen van zonne-bestralingssterkten gemeten in het ultraviolet en in het uiterst ultraviolet. Verschillende voorbeelden van absorptieprofielen en ionenproductie verhoudingen worden besproken voor veranderlijke voorwaarden. Verscheidene energetissche effecten werden eveneens beschreven. Al de berekeningen werden gemaakt voor fysische voorwaarden boven Scheveningen (52°08N) waar het 14e ESLAB symposium werd gehouden.

Zusammenfassung

Verschiedene semi-empirische Modellen der erdischen höheren Atmosphäre sind zurzeit disponibel. Diese Modellen führen Rechnung über die Sonnenaktivität mit Hilfe der Sonnendecimetrischestrahlung als Index. Solche Methode folgt aus dem Mangel an durchlaufenden Messungen des Sonnenspektrum vorantwörtlich für die physikalische Struktur der höheren Atmosphäre. Variationen der Temperatur zur Thermopause sind diskutiert. Fünf Messungen der UV und EUV Sonnenstrahlung werden gebraucht um die Durchschlagskraft der Sonnenstrahlung für verschieden Sonnenaktivitäten zu analysieren. Beispiele der Absorption und der Ionenproduktion werden für veränderlichen Bedingungen vorgestellt. Verschiedene energetische Effekten sind auch beschrieben. Die Rechnungen sind gültig für physikalischen Bedingungen über Scheveningen (52°.08N) wo das 14. ESLAB Symposium stattgefunden hat.

INTRODUCTION

Soon after 1900 it became progressively clear that the propagation of wireless waves is influenced by ionized particles in the upper atmosphere. Around 1925, the ionizing agent was tentatively attributed to solar ultraviolet radiation. The absence of direct measurements of this radiation, the lack of laboratory data on absorption cross sections and recombination coefficients and the poor knowledge of the upper atmosphere composition lead to several contradictory explanations. The early ionospheric investigations described by Bates (1973), Waynick (1975) and Ratcliffe (1978) are, however, a first milestone for our understanding of the upper atmosphere. Ground based radio propagation experiments remained a unique technique until the advent of space vehicles.

The first ultraviolet solar spectrum down to 240 nm was recorded at 55 km altitude on October 10, 1946 using a V-2 rocket (Baum et al. 1946) and Johnson et al. (1952) observed shorter wavelengths above 100 km in 1949. These experiments opened a new area for upper atmosphere research, since they proved the existence and the measurement feasability of the short wavelength part of the solar spectrum. Since that time, significant progress has been achieved in the measuring techniques which will not be discussed here. The primary objective of this paper is to stress the importance of reliable solar ultraviolet data for a quantitative understanding of the physical phenomena occuring in the upper atmosphere. Such an objective is sometimes in conflict with the primary interest of solar physicists since they may consider the Earth's atmosphere as an obstacle. It is, however, suitable to know the structure and the behavior of an obstacle if one wants to avoid it.

As a consequence the behavior of the upper atmosphere as a function of solar activity is discussed in the framework of the limited amount of solar ultraviolet data presently available.

2. SOLAR ACTIVITY AND TEMPERATURE OF THE THERMOSPHERE

After the launching of the first artificial satellites, Jacchia (1959), Groves (1959), Priester (1959), and King-Hele and Walker (1959) showed almost simultaneously that the apparently erratic fluctuations of the orbital periods are a direct consequence of total density variations in the upper atmosphere. Satellite drag data actually lead to a determination of the atmospheric total density in the vicinity of the satellite perigee. Variations of the total density at a given height may result from composition changes and/or temperature modifications. Above the mesopause, near 85 km altitude, molecular oxygen is photo-dissociated by solar radiation with wavelengths shorter than 175 nm and atomic oxygen becomes progressively more abundant than O_2 and N_2 as a consequence of diffusive separation in the Earth's gravitational field. Furthermore, diffusive transport is such that two minor constituents at the mesopause, namely helium and atomic hydrogen, become successively the most abundant components above 500 km altitude. In such an over-simplified picture, the terrestrial thermosphere is characterized by four belts in which molecular nitrogen, atomic oxygen, helium and atomic hydrogen are successively the most abundant constituents (Kockarts and Nicolet, 1962; 1963). For a given temperature profile, the vertical variation of the total density is, however, insufficient to explain the observed drag data over a long period of time. It is actually necessary to introduce temperature variations which also affect the atmospheric composition. Temperature variations can be induced by particle transport processes, by day to night variations and by changes of the external heat sources. The importance of molecular heat conduction and of external heat sources were indicated by Lowan (1955) and Johnson (1956) in several attempts to construct thermospheric models. Detailed calculations of theoretical models are extremely difficult, since they require a simultaneous solution of continuity, momentum and energy conservation equations. Even with an appropriate mathematical technique, it is still necessary to make use of experimental results for

upper and lower boundary conditions. Solar ultraviolet fluxes below 175 nm are among the most important boundary conditions and these data should be available for all solar activity conditions.

Present thermospheric models are, however, based on an empirical approach partially justified by the lack of continuous solar ultraviolet flux measurements and by the mathematical difficulties to solve the coupled conservation equations. Several types of vertical temperature profiles are commonly used in thermospheric modelling. A pratical profile which allows an analytical expression for the vertical distributions of the atmospheric constituents was introduced by Bates (1959). It should be realized that this profile is not a solution of the heat conduction equation. Therefore, it can only be considered as an approximation. Such a profile depends on the thermopause temperature, on the lower boundary temperature at 120 km and on a shape parameter which relates these two quantities to the temperature gradient at the lower boundary altitude. With given shape parameter and lower boundary temperature it is possible to establish an analytical relation $\rho(z) = f(T_\infty, z)$ between the total density $\rho(z)$ at height z and the thermopause temperature T_∞. Determining T_∞ remains then the fundamental problem. Collecting all nighttime total densities near 4 to 5 hours local solar time and searching to which thermopause temperature they correspond, one can establish an empirical relation between the thermopause temperature and a parameter reflecting the solar activity level. In all semi-empirical thermospheric models, solar activity is represented by the 10.7 cm radioelectric flux measured regularly at Ottawa. This decimetric flux has no influence on the thermal structure of the upper atmosphere. When the solar decimetric flux is averaged over several solar rotations, usually three, the long term variation of the thermopause temperature $T_\infty(1)$ is given by

$$T_\infty(1) = a + b\,\bar{F} \qquad (1)$$

where $\bar{F}$ is the daily solar decimetric flux in units of 10^{-22} Wm^{-2} Hz^{-1}

averaged over three solar rotations and a and b are model dependent numerical coefficients.

The 27 days variation is taken into account by correcting expression (1) in a way such that

$$T_\infty(2) = T_\infty(1) + c(F - \bar{F}) \qquad (2)$$

where F is the daily 10.7 cm solar flux taken one day before the day to which $T_\infty(2)$ corresponds. A third approximation is obtained by correcting $T_\infty(2)$ for a geomagnetic effect associated with particle precipitations and or Joule heating. In this case,

$$T_\infty(3) = T_\infty(2) + \Delta T \qquad (3)$$

where ΔT is essentially a function of the geomagnetic index in the first thermospheric models (Jacchia, 1965). The temperature increase ΔT is not associated with solar ultraviolet flux variations. Roemer (1971) has shown that the geomagnetic effect depends on the latitude. A fourth correction intends to represent the semi-annual variation observed in the total density such that the thermopause temperature is given by

$$T_\infty(4) = T_\infty(3) + f(t) \qquad (4)$$

where f(t) is a function of the day count in the year. Such a procedure was used by Jacchia (1965) to obtain a nighttime minimum temperature and the diurnal variation was then estimated from a one-dimensional theoretical calculation of Harris and Priester (1962).

A functional relation like expression (4) combined with constant boundary conditions at 120 km and the diffusion equilibrium hypothesis, implies that any temperature variation induces instantaneously a modification of the total density. In situ measurements have shown that

composition changes are not necessarily associated with temperature changes. As an example, Champion (1967) has shown that a seasonal-latitudinal variation of the total density exists in the lower thermosphere below 200 km and Keating and Prior (1968) observed a strong increase of helium concentration above the winter pole as compared to the local summer value. With such considerations a new set of models (Jacchia, 1971) was constructed and adopted as the COSPAR International Reference Atmosphere (CIRA, 1972). Lower boundary conditions are now taken at 90 km; a departure from diffusive equilibrium is introduced for atomic and molecular oxygen between 90 km and 120 km; the geomagnetic effect is latitude dependent and associated simultaneously with a temperature variation and a total density variation; the semi-annual effect is represented as a correction to the total density; and, the diurnal variation of the thermopause temperature is given by an empirical expression.

Two important aspects are, however, not covered by these improvements. First of all, temperature determinations from incoherent scatter observations (Carru et al. 1967; Nisbet, 1967) clearly indicate that the thermopause temperature peaks later than the 14 hours local solar time maximum of the total density. This important contribution is only taken into account in very recent models and specific models are now available for Saint-Santin (44.6°N) (Bauer et al. 1970) and for Millstone Hill (42.6°N) (Salah et al. 1976). Furthermore, OGO-6 mass spectrometer observations (Mayr et al. 1974) have shown that the partial density of each constituent reaches a maximum value at a local time which depends on the altitude and on the constituent.

Since the description of the terrestrial thermosphere is becoming more complex as it approaches physical reality, Jacchia (1977) developed a new set of models consisting of two parts : static models and a set of empirical expressions to compute the thermopause temperature and the expected deviations from the static models resulting from all recognized thermospheric variations. The formulation is, however, more com-

plicated, since any new refinement must not destroy the previous achievements.

A completely different approach has been made by Hedin et al. (1974) who used spherical harmonics for a global representation of mass-spectrometric data. In a very general case, one writes

$$T_\infty = \bar{T}_\infty \, G_1 \tag{5}$$

$$T_{120} = \bar{T}_{120} \, G_2 \tag{6}$$

$$s = \bar{s} \, G_3 \tag{7}$$

$$n_i(120) = \bar{n}_i(120) \exp (G_i - 1) \tag{8}$$

where T_∞ is the thermopause temperature, T_{120} is the temperature at 120 km, s is the shape parameter in the analytical temperature profile given by Bates (1959) and n_i (120) is the concentration of constituent i at 120 km altitude. G_1, G_2, G_3 and G_i are spherical harmonics expansions which depend on latitude, local solar time, geomagnetic index K_p or A_p, daily solar decimetric flux F, solar decimetric flux $\bar{F}$ averaged over three solar rotations and day count in the year. $\bar{T}_\infty$, $\bar{T}(120)$, $\bar{s}$ and $\bar{n}_i(120)$ are averaged values of the respective quantities, when the corresponding G function is one. Formal expressions G_1 to G_i slightly vary from one aouthor to another. Several semi-empirical models based on spherical harmonics are presently available (Hedin et al. 1977a, 1977b; von Zahn et al. 1977; Barlier et al. 1978; Köhnlein, 1980). All these models allow a computation of the thermopause temperature at any place over the globe as a function of solar activity, geomagnetic activity, local solar time and day count in the year. Comparisons between various models have been made by Barlier et al. (1977), by Jacchia (1979) and by Kockarts (1981). For very low ($\bar{F}$ = 70 x 10^{-22} Wm^{-2} Hz^{-1}) or very high ($\bar{F}$ = 200 x 10^{-22} Wm^{-2} Hz^{-1}) the

resulting daily averaged thermopause temperature can vary by approximately 100 K depending on the adopted semi-empirical model.

Figures 1a and 1b give the thermopause temperature above Scheveningen (52.08°N) between 1958 and 1980. Computations are made at 17 hours LST (local solar time) on the first of each month. The adopted LST approximately corresponds to time of the daily temperature maximum. Vertical dotted lines show the temperature increase resulting from geomagnetic activity. The full line in the lower part indicated the 10.7 cm solar flux $\bar{F}$ averaged over three solar rotations whereas the dashed line gives the daily solar decimetric flux F taken the day before the first of each month as required by the model of Barlier et al. (1978). This model, called DTM (Drag Temperature Model) is based on satellite drag data and on a temperature model constructed by Thuillier et al. (1977) from Fabry-Perot interferometer measurements of spectral profiles of the 630 nm airglow line as observed on OGO-6 by Blamont and Luton (1972). Incoherent scatter data are also included in the temperature model. Temperature data were obtained from 8 June 1969 to 16 August 1970 as indicated by the horizontal line in Figure 1b. The DTM model is adopted here since it is the sole semi-empirical model which is constructed with optically measured temperatures. In all other semi-empirical model thermopause temperatures are quantities deduced in a way as to fit measured concentrations or total densities. Optical determinations are presently the sole technique used to determine directly global temperature coverage, since the incoherent scatter technique is unfortunately restricted by the limited amount of incoherent scattering stations. Furthermore, Fabry-Perot interferometer measurements are limited up to now to a very short time period as it can be seem in Figure 1b. From an absolute point of view, all temperatures in Figures 1a and 1b before June 1969 and after August 1970 are extrapolations ! However, these temperatures lead to concentrations and total densities in reasonable agreement with mass spectrometer data and satellite drag data.

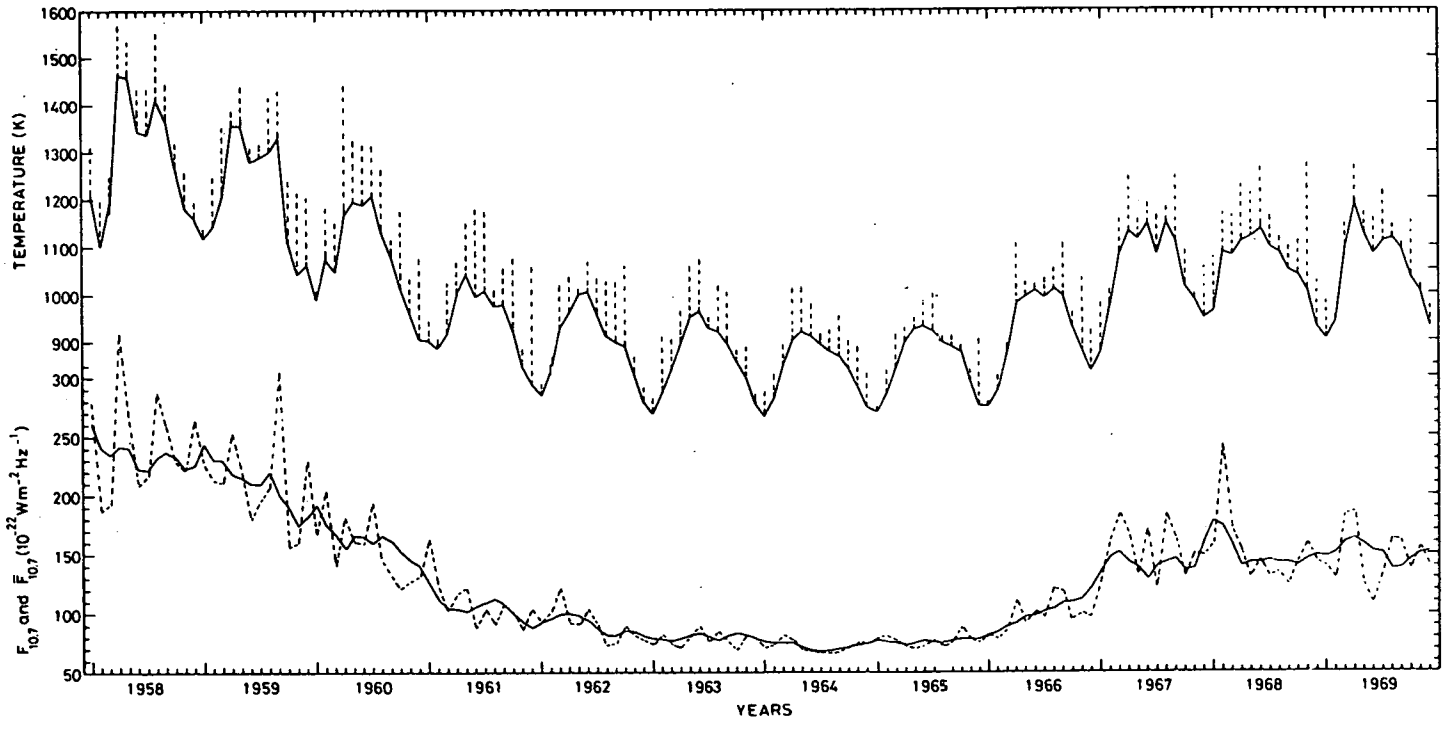

Fig. 1a : Thermopause temperature at 17 hours LST above Scheveningen (52.08°N) on the first of each month from 1958 to 1969. Vertical dashed line indicate temperature increases resulting from geomagnetic activity. Dashed curve in the lower part gives the daily 10.7 cm solar flux $F_{10.7}$ in 10^{-22} Wm^{-2} Hz^{-1}; full curve represents the averaged value $\bar{F}_{10.7}$ over three solar rotations.

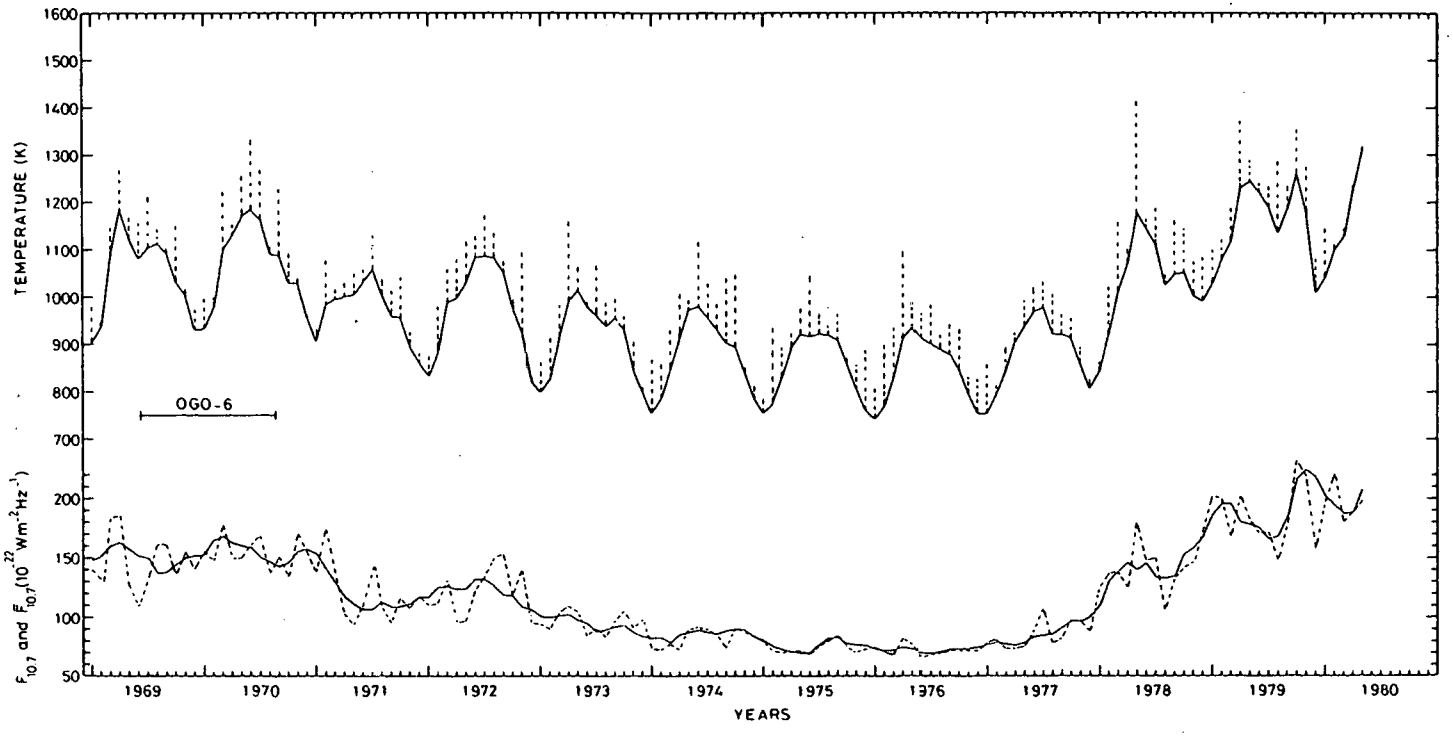

Fig. 1b : Continuation of Fig. 1a from 1969 to 1980. Horizontal line labeled OGO-6 indicate the time period over which temperature data were measured with a Fabry-Perot interferometer.

Several interesting features can be seen in Figures 1a and 1b. The variation of the thermopause temperature with the 11 years solar cycle is clearly apparent. Furthermore, two consecutive solar cycles are not necessarily identical. As an example, the thermopause temperature was much higher during the 1958 maximum than during the 1969 maximum, which seems to be lower than the 1980 maximum. An annual variation appears in the temperature and it is not correlated with the solar decimetric flux. Therefore, a higher solar decimetric flux can correspond to a lower temperature, depending on the day in the year. Peaks in the daily flux F do not necessarily lead to peaks in the thermopause temperature which cannot be considered as directly proportional to F or $\bar{F}$ or a combination of both.

3. GLOBAL TEMPERATURE AND TERRESTRIAL INSOLATION

In the DTM model of Barlier et al. (1978) the spherical harmonics expansions used in expressions (5) to (8) are formally given by

$$G = 1 + F_1 + M + \sum_{q=1}^{\infty} a_q^o P_q^o(\theta) + \beta \sum_{p=1}^{\infty} b_p^o P_p^o(\theta) \cos [p\,\Omega(d - \delta_p)]$$

$$+ \beta \sum_{n=1}^{\infty} \sum_{m=1}^{\infty} \{ c_n^m P_n^m(\theta) \cos (m\omega t) + d_n^m P_n^m(\theta) \sin (m\omega t)\} \quad (9)$$

where $P_n^m(\theta)$ are associated Legendre functions of the colatitude θ, $\Omega = 2\pi/365$ (day^{-1}) and $\omega = 2\pi/24$ (hour^{-1}). The solar decimetric flux dependence and the geomagnetic effect are respectively given by F_1 and M. Coefficient β is $1 + F_1$, d is the day count in the year and t is the local solar time. The development (9) is limited such that 35 unknown coefficients must be determined by a least square technique. It should be noted that the form of some terms in expression (9) is chosen a priori before a least square is used to determine the unknown coefficients. This is the case for the solar activity effect given by

$$F_1 = A_4 (F - \bar{F}) + A_5 (F - \bar{F})^2 + A_6 (\bar{F} - 150) \quad (10)$$

where the decimetric fluxes F and $\bar{F}$ are measured in units of 10^{-22} Wm^{-2} Hz^{-1} and for the geomagnetic activity effect given by

$$M = (A_7 + A_8 P_2^o(\theta)) K_p \qquad (11)$$

where K_p is the three-hourly planetary index taken 3 hours before the considered local solar time.

When $F = \bar{F} = 150$ and $K_p = 0$ expressions (5) and (9) lead to a global temperature distribution which only depends on annual, semi-annual and diurnal variations. The last effect can also be eliminated by integration over the 24 hours day period. A global diurnally averaged temperature distribution can be computed as shown in Figure 2 where thermopause temperature isopleths are given as a function of geographic latitude and day count in the year. Such a map shows a pronounced seasonal variation in both hemispheres. This variation is independent of a modification in the decimetric flux ($F = \bar{F} = 150$ = constant through the year) or in K_p kept always equal to zero. Such a hypothetical case can be used to make a comparison with the daily averaged insolation which should be at least partially responsible for a seasonal variation.

According to Milankovitch (1930), the daily averaged insolation $\bar{I}$ on a horizontal surface at latitude φ for a solar declination δ is given by

$$\bar{I} = I_a \pi^{-1} (a/r)^2 (\psi_o \sin \varphi \sin \delta + \sin \psi_o \cos \varphi \cos \delta) \qquad (12)$$

where I_a is the solar flux at 1 AU = a, r is the actual Sun-Earth distance and $\psi_o = - \operatorname{tg}\varphi \operatorname{tg} \delta$. For regions with permanent sunlight $\psi_o = \pi$ and during polar night $\psi_o = 0$. Application of expression (12) leads to the isopleths shown in Figure 3 computed for an arbitrary incident flux $I_a = 1$. Values of $\bar{I}$ are given on each curve. Solar declination is indicated by the dashed line and limits of polar nights are shown by dotted-dashed lines. Figure 3 can be applied to any solar ultraviolet

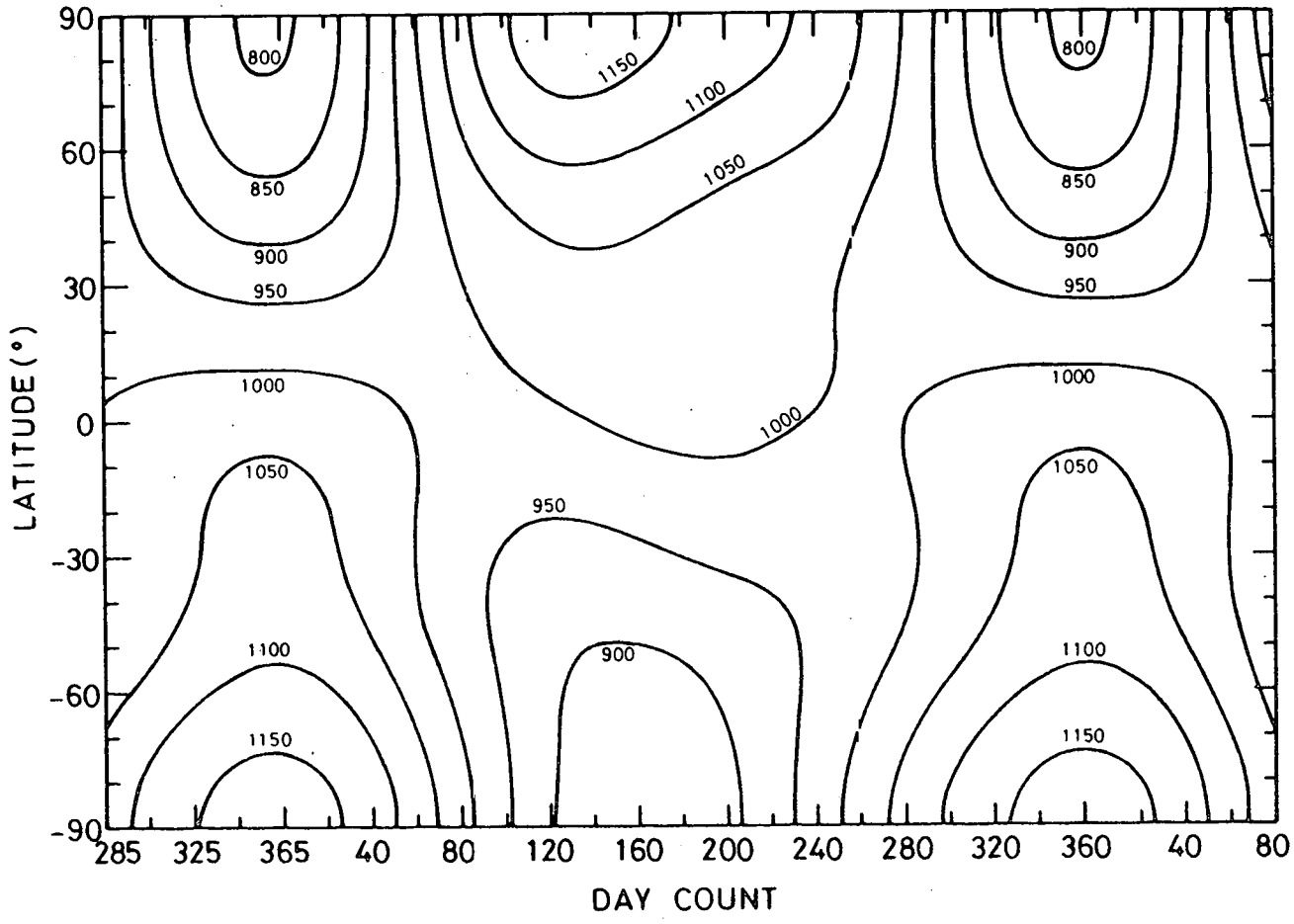

Fig. 2 : Isopleths of daily averaged thermopause temperature for $F_{10.7} = \bar{F}_{10.7} = 150 \times 10^{-20}$ $Wm^{-2}Hz^{-1}$ and $K_p = 0$.

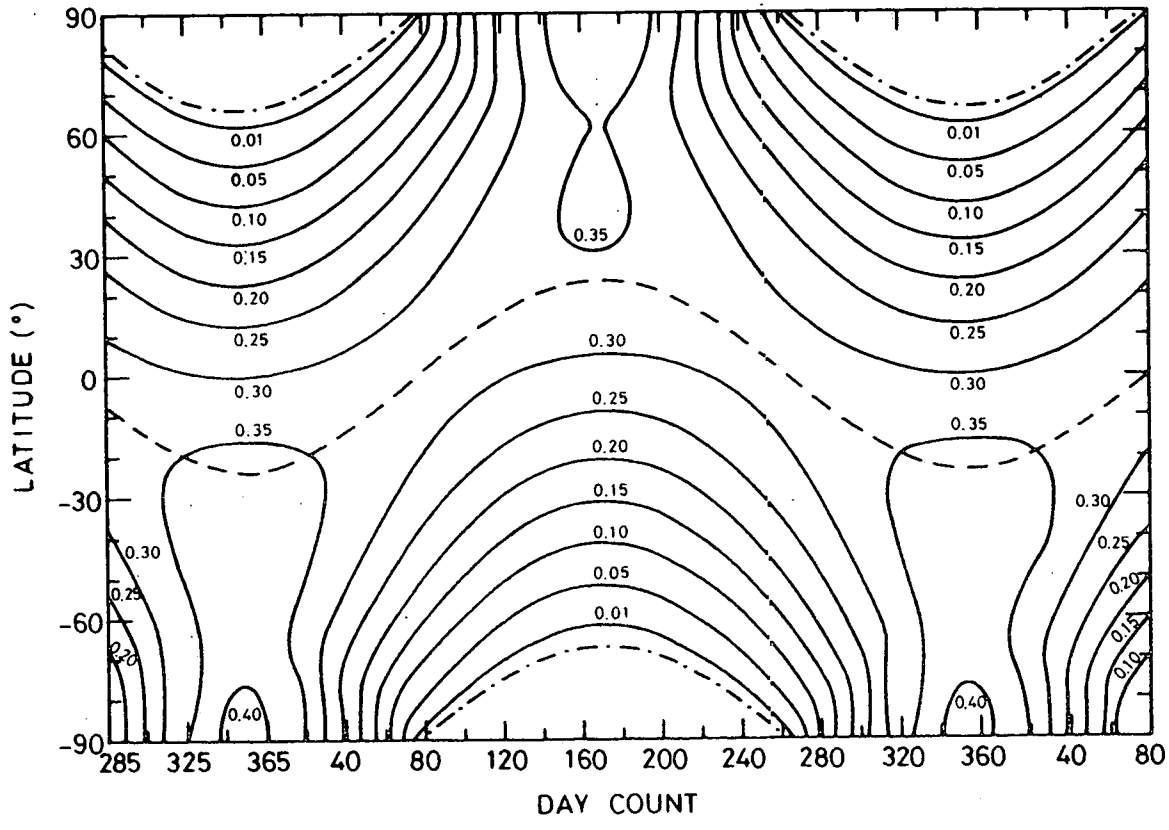

Fig. 3 : Isopleths of daily averaged insolation for an arbitrary solar irradiance I_a = 1 at 1 A.U. Solar declination is given by the dashed line and permanent polar nights are indicated by dotted-dashed lines.

flux reaching a horizontal surface at the top of the atmosphere before absorption processes become effective. Daily averaged values are obtained by multiplying solar ultraviolet fluxes by the numbers on each isopleth. Figures 2 and 3 have some obvious similarities indicating that the geometry of the insolation plays a significant role in the global structure of the thermopause temperature. Furthermore, both Figures show a definite North-South asymmetry : during local summer the temperature is higher in the southern hemisphere which receives also more solar energy than the northern hemisphere. Such asymmetries exist also in the thermospheric composition (Barlier et al. 1974), but no quantitative explanation has been given.

Figures 2 and 3 are superimposed in Figure 4 in order to show the relation between insolation and thermopause temperature. In the southern hemisphere the local summer maximum of the thermopause temperature corresponds rather well with the maximum insolation. However, in the northern hemisphere the maximum temperature occurs before maximum in-solation. The partial similarity between both types of isopleths in Figure 4 is, nevertheless, an indication to justify another semi-empirical representation as given by expression (9). Since the instantaneous as well as the daily averaged illumination are known analytically it could be rewarding to introduce them in expression (9) for a better representation of the effect of solar ultraviolet radiation.

When the daily mean temperature is averaged in each hemisphere one obtains the result shown in Figure 5 which gives also the daily mean insolation as a function of the day count in the year. The North-South asymmetry appears very clearly in the mean hemispheric temperature. However, it should be noted that the annual mean temperature as well as the annual mean insolation are identical in both hemispheres.

No ultraviolet solar flux data are included in any semi-empirical model, but this does not imply that much better models can be constructed without such data. The 10.7 cm decimetric flux is commonly

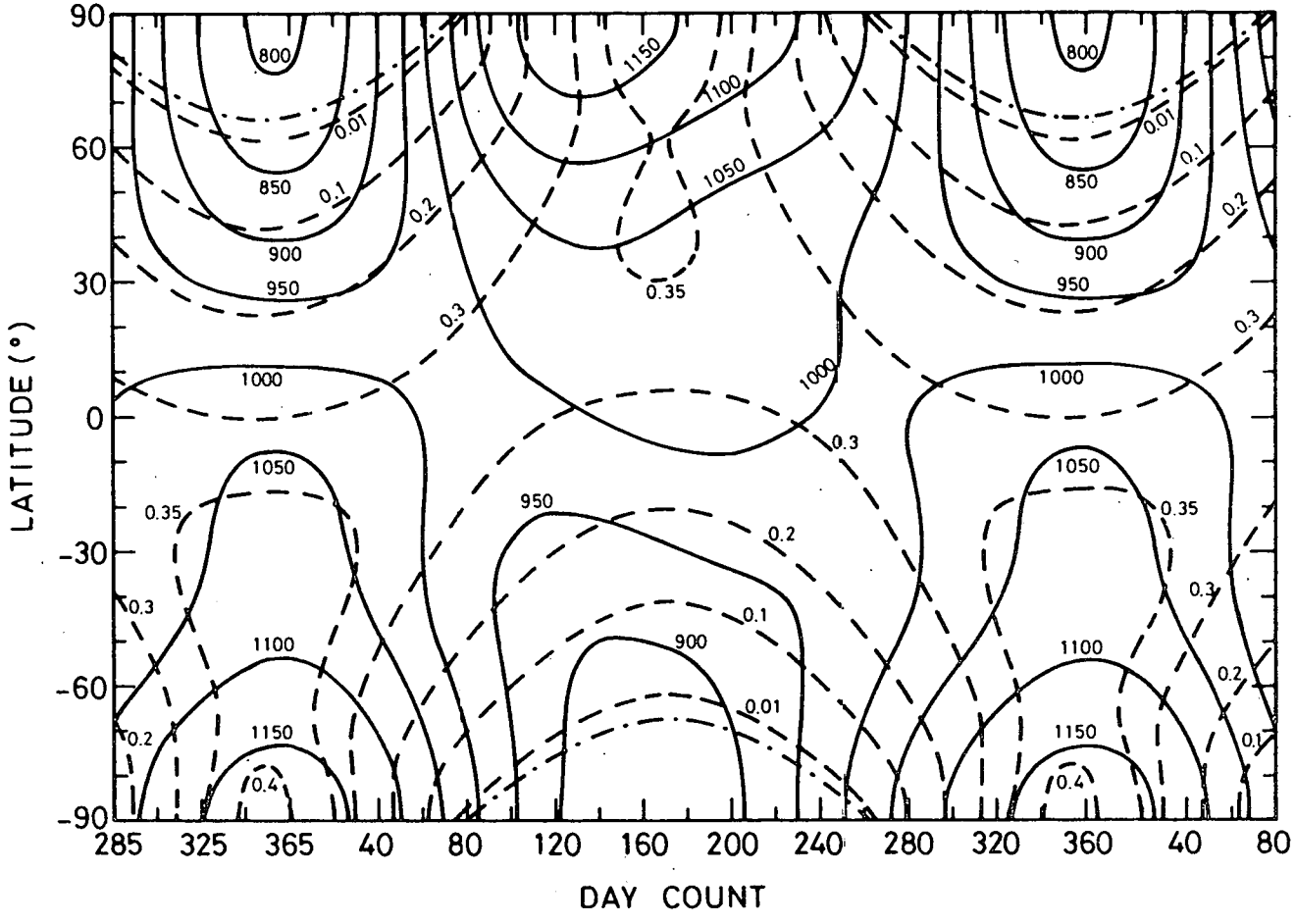

Fig. 4 : Superposition of Figs. 2 and 3 in order to show a correlation between insolation (dashed lines) and temperature (full lines).

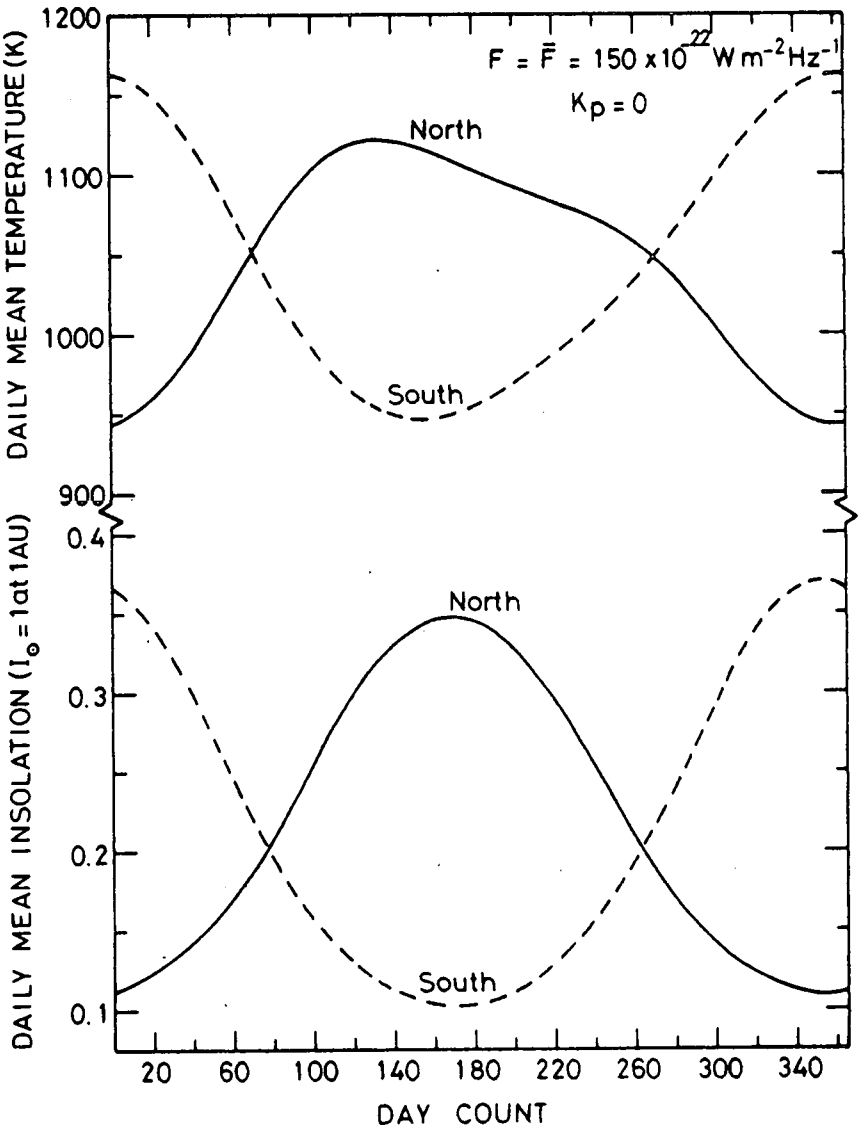

Fig. 5 : Daily mean thermopause temperature averaged over northern (full curve) and southern (dashed curve) hemisphere. Relative daily mean insolation is given in the lower part.

used, since no better index is presently available to represent variations of solar ultraviolet fluxes responsible for the highly variable state of the terrestrial upper atmosphere.

4. PENETRATION OF SOLAR RADIATION

Before estimating effects of solar ultraviolet radiation on the terrestrial atmosphere, it is necessary to know how deeply any solar radiation can penetrate into the atmosphere. The best quantity to make such an estimation is the optical depth defined by

$$\tau(\lambda,\chi,z) = \sum_i \sigma_i(\lambda)\, n_i\, H_i\, Ch\,(\chi,z) \qquad (13)$$

where χ is the solar zenith distance, $\sigma_i(\lambda)$ is the absorption cross section at wavelength λ for the i-type atmospheric constituent with concentration n_i and scale height H_i at altitude z. $Ch(\chi,z)$ is simply the secant of the solar distance when χ is smaller than 75°. For larger distances Chapman (1931) has shown that the Earth's curvature must be taken into account and various analytical approximations are available for the Chapman function $Ch(\chi,z)$ (Swider, 1964; Swider and Gardner, 1969).

As a consequence of the exponential decrease of the atmospheric constituents, maximum of absorption approximately occurs at the altitude where $\tau(\lambda,\chi,z) = 1$. Using the semi-empirical model DTM of Barlier et al. (1978) and the absorption cross sections tabulated for 5 nm wavelength intervals by Torr et al. (1979) between 5 nm and 105 nm, one obtains in Figure 6 the altitudes where unit optical depth is reached as a function of wavelength. Computations are made for 12 hours LST above Scheveningen for specific days when solar ultraviolet fluxes are available in tabular form. Above 105 nm molecular oxygen absorption cross sections are adopted as averaged values of the detailed measurements of Ogawa and Ogawa (1975). These values are in reasonable agreement with the averaged cross sections suggested by Ackerman

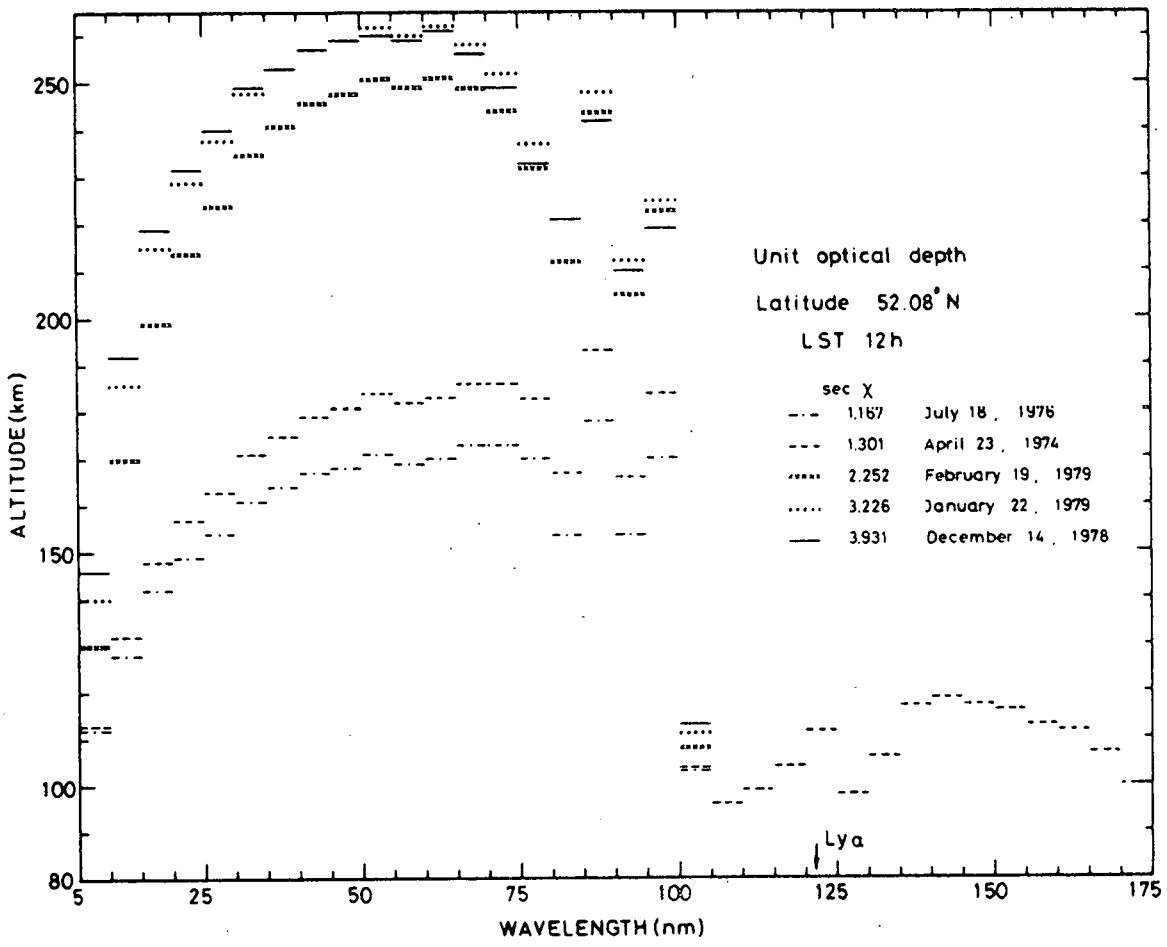

Fig. 6 : Altitude for unit optical depth as a function of wavelength. Computations are made at 12 hours LST above Scheveningen for five days.

(1971). Since semi-empirical models usually do not extend below 120 km altitude, the U.S. Standard Atmosphere for 45°N was used below that height with some arbitrary ajustment to match the concentrations given by DTM at 120 km. It can be seen in Figure 6 that the height for unit optical depth strongly depends on the wavelength, on the solar zenith distance and on solar activity. Although no solar flux value enters in the computation of the optical depth, the neutral atmosphere above 120 km is sufficiently variable with solar activity to modify the height were maximum absorption occurs. Solar activity variations induce strong modifications in the composition and temperature of the upper atmosphere and it is completely unrealistic to adopt a unique curve for the altitude of unit optical depth. Furthermore, seasonal and diurnal variations also affect the penetration of solar radiation.

Solar ultraviolet fluxes corresponding to the dates indicated in Figure 6 were measured on board of Atmosphere Explorer E and are tabulated by Torr et al. (1979) below 105 nm. Figure 7 shows the extreme values corresponding to high solar activity (19 February 1979) and to low solar activity (23 April 1974). Dots and crosses correspond to solar emission lines whose intensities are included in the flux values averaged over 5 nm intervals. Above 105 nm the height of unit optical depth is only given for 23 April 1974 since tabulated flux values are only available for this date (Heroux and Hinteregger, 1978) at the present time. Hopefully more data will become available very soon, since the lower thermosphere between 85 km and 120 km is still poorly known. Good solar irradiance data in the Schumann-Runge continuum below 175 nm are of paramount importance, since molecular oxygen is strongly photodissociated in this wavelength range in the lower thermosphere and leads to atomic oxygen which becomes a major atmospheric constituent above 150 km altitude. Comparisons between atomic oxygen concentrations at 120 km from semi-empirical models and from optical measurements reveal discrepancies which may reach a factor of four (Kockarts, 1981).

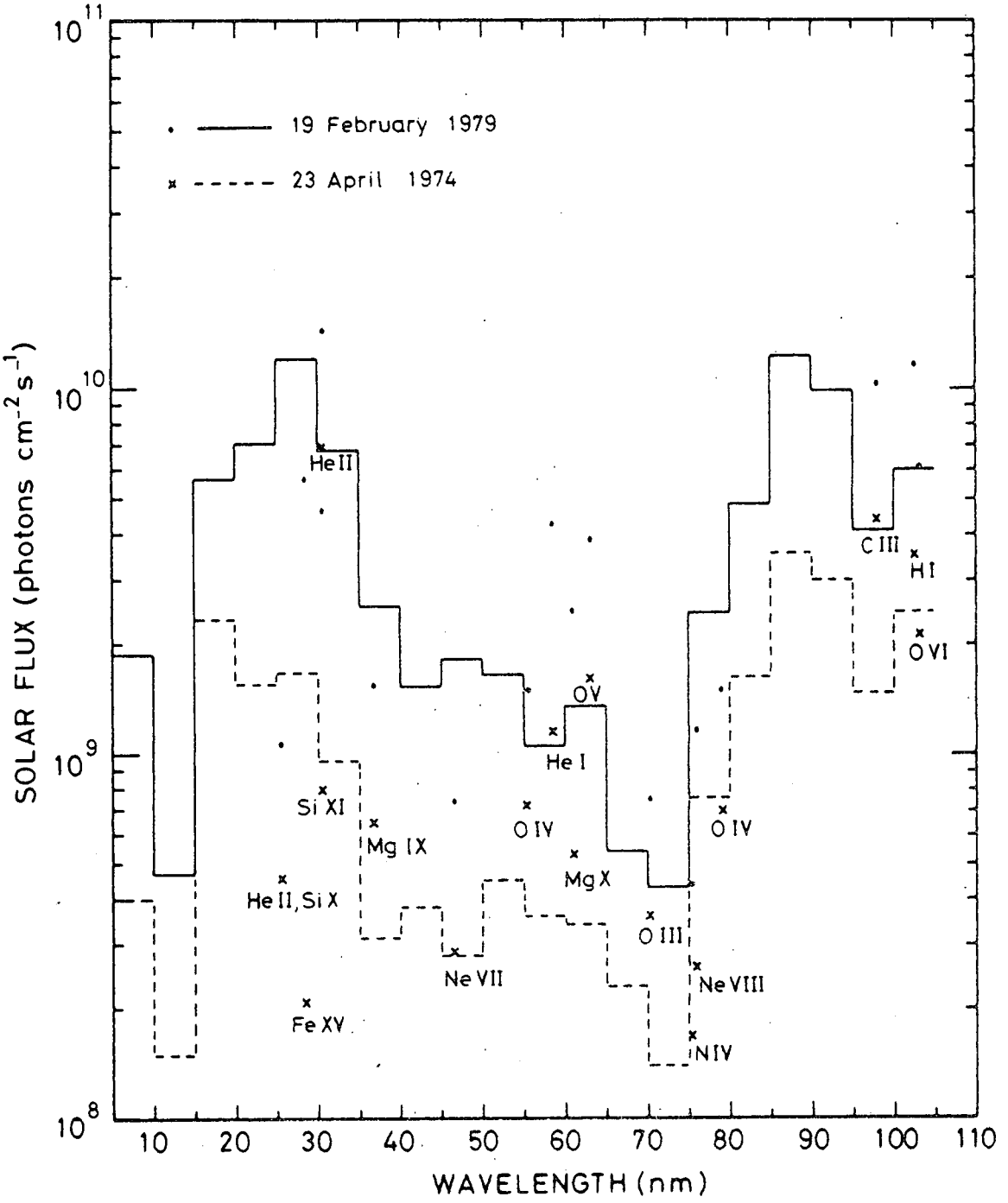

Fig. 7 : Extreme values of solar irradiances between 5 nm and 105 nm corresponding to minimum (23 April 1974) and to maximum (19 February) solar activity conditions. Dots and crosses correspond to solar emission lines included in the 5 nm intervals averaged values.

Whereas semi-empirical atmospheric models use only two solar activity indices (F and $\bar{F}$), solar ultraviolet fluxes measurements deal with more than 1000 individual wavelengths. Hinteregger (1981) discussed various representations of solar fluxes for aeronomical applications. There is actually no universal solution, since the adopted wavelength intervals depend on the objective which has to be tackled. On one hand the solar spectrum has its own characteristics and on the other hand the atmospheric species have their individual absorption spectra. The cross sections tabulated by Torr et al. (1979) at 5 nm wavelgnth intervals are weighted values computed from a compilation by Kirby et al. (1979) at all wavelengths of the solar lines and continua given in a solar reference spectrum of Hinteregger (1976). Molecular oxygen and molecular nitrogen have complicated absorption and ionization cross sections (see Banks and Kockarts, 1973a; Lofthus and Krupenie, 1977) which are not always perfectly known.

As stated previously the optical depths used in Figure 6 are computed with 5 nm interval averaged molecular oxygen absorption cross sections between 105 nm and 175 nm. Measured absorption cross sections (Ogawa and Ogawa, 1975) are shown in Figure 8 for the ground state $O_2(X^3\Sigma_g^-)$. The strong band structure below 130 nm clearly indicates that a detailed analysis of the penetration of solar radiation would require a much higher resolution of the solar spectrum. Incidentally, the small absorption cross section of O_2 at Lyman-α indicates why this radiation can penetrate in the terrestrial atmosphere down to mesospheric levels. Lyman-α line at 121.567 nm is not included in the unit optical depth computation of Figure 6.

Another interesting example is given by the highly variable absorption cross section of O_2 in the Schumann-Runge bands. Using the absorption cross sections of Ackerman et al. (1970) it is possible to estimate the structure of the solar spectra which could be observed at 85 km altitude for 90° solar zenith distance. The results of such a computation is shown in Figure 9 for the 10-0 band. The incident solar

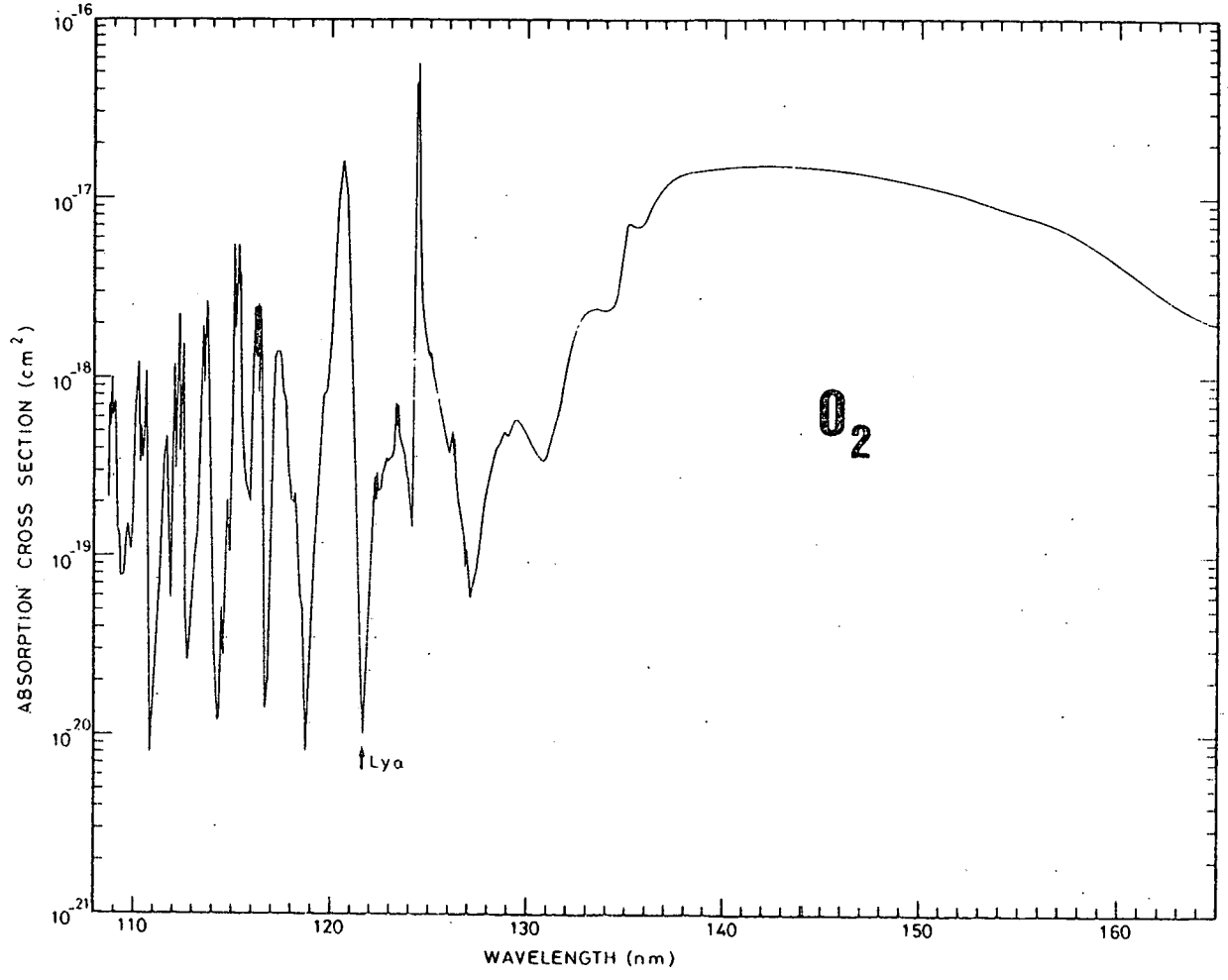

Fig. 8 : Absorption cross section of ground state molecular oxygen between 109 nm and 165 nm.

irradiance, shown in the upper part of Figure 9, is taken from Samain and Simon (1976). It appears that the incident spectrum is strongly modified and the resulting spectrum is even temperature dependent since the absorption cross section in the Schumann-Runge bands is influenced by the atmospheric temperature. Such an experiment could provide informations not only on the solar spectrum, but also on the absorption spectrum of molecular oxygen. A first approach along this line has been made by Longmire et al. (1979) during re-entry of a rocket launched from the White Sands, New Mexico, missile range. Other examples showing how the optical depth varies in several bands of the Schumann-Runge system are given by Kockarts (1971). In photochemical models dealing with numerous chemical reactions and transport phenomena, it is, however, difficult to introduce the detailed absorption in the Schumann-Runge bands. Therefore, several simple approximations have been established (see Kockarts, 1976) in order to provide a convenient technique for the computation of solar penetration in the Schumann-Runge bands of molecular oxygen.

5. ENERGETIC EFFECTS OF SOLAR RADIATION

Any consideration of the effect of solar radiation on the terrestrial atmosphere should deal with three aspects : the intensity of the solar radiation, the capability for atmospheric species to absorb this radiation and the abundance of the absorbing species. With, the tabulated values of Torr et al. (1979) for solar irradiances between 5 nm and 105 nm and the values of Heroux and Hinteregger (1978) between 105 nm and 175 nm, the atmospheric model of Barlier et al. (1978) leads to the absorbed energy rates above Scheveningen shown in Figure 10 for 12 hours LST on the day when the solar fluxes were measured. The U.S. Standard Atmosphere was used below 120 km altitude. The full curve gives the total energy absorbed between 5 nm and 175 nm. The dashed, dotted-dashed and dotted curves are the contributions of the indicated wavelength ranges to the total absorption. Lyman-α is not included in the 105-135 nm interval, since this radiation is only absorbed below

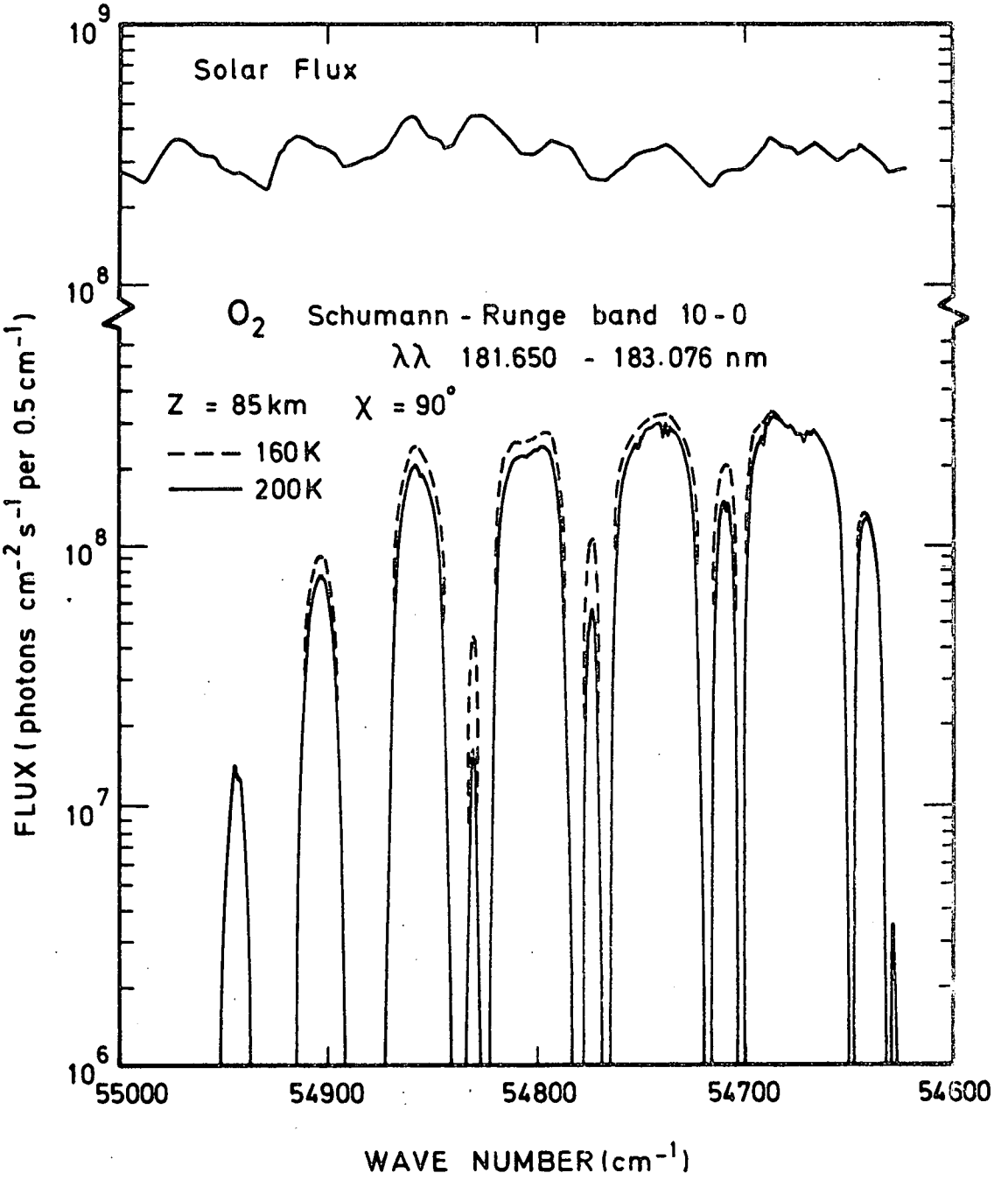

Fig. 9 : Penetration of solar radiation in the 10-0 band of the Schumann-Runge system of O_2. Grazing incidence (χ = 90°) is assumed at 85 km altitude where two extreme temperatures are adopted. Incident solar flux is shown in the upper part.

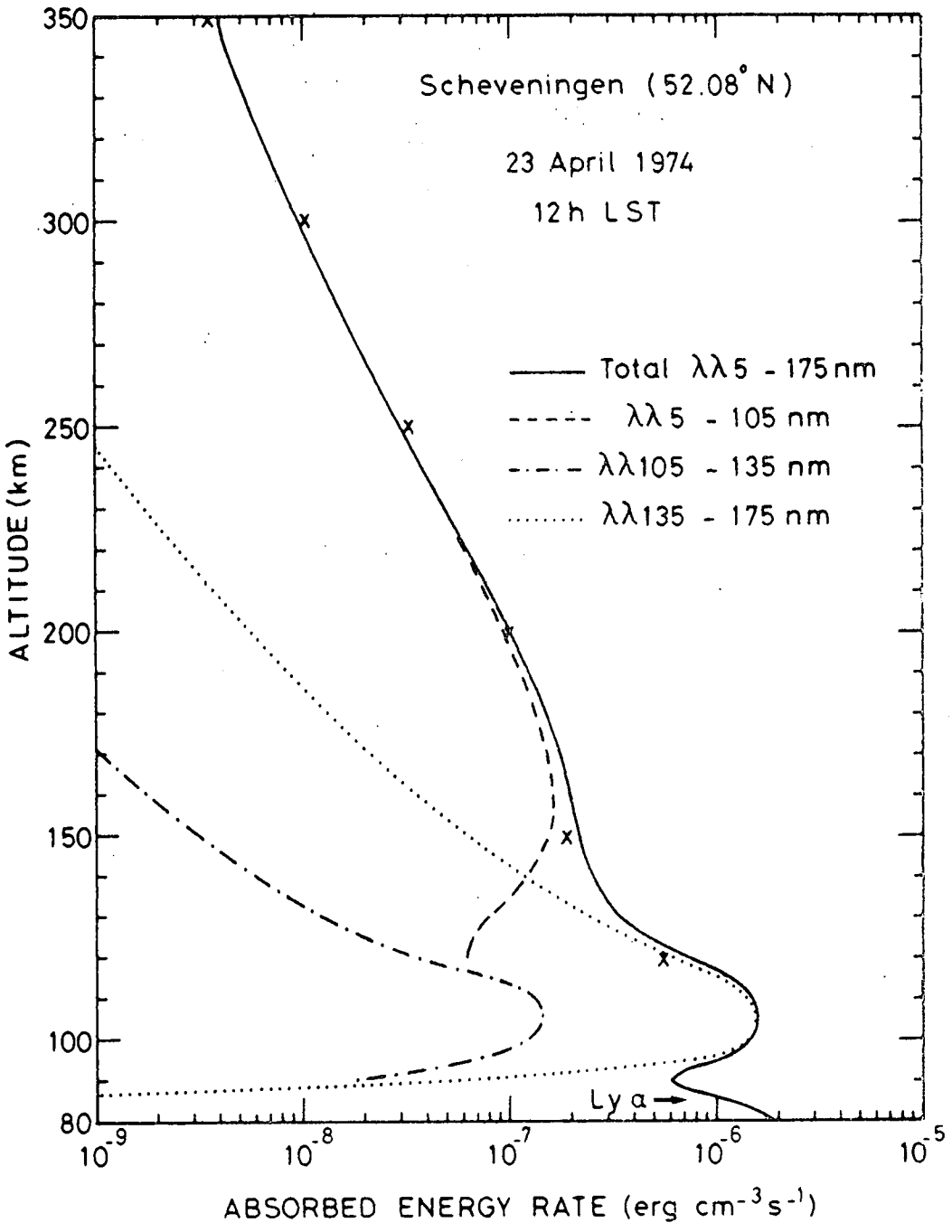

Fig. 10 : Absorbed energy rate as a function of height at 12 hours LST on 23 April 1974 above Scheveningen. Energy distribution in various wavelength ranges is shown by dashed line, dotted line and dotted dashed line.

100 km as a consequence of the low absorption cross section of O_2 (see Figure 8) at 121.567 nm. It can be seen that the extreme ultraviolet wavelength range ($\lambda\lambda$ 5-105 nm) is mainly absorbed above 150 km, whereas absorption in the Schumann-Runge continuum ($\lambda\lambda$ 135-175 nm) peaks around 100 km and Lyman-α has its maximum absorption in the mesosphere below 85 km altitude. The wavelength range $\lambda\lambda$ 105 - 135 nm corresponds to a highly variable absorption cross section for O_2 (see Figure 8) but the absorbed energy rate has been computed with averaged cross sections. Crosses in Figure 10 indicate total absorbed energy rates obtained when the neutral model of Hedin et al. (1977a, b) is used instead of DTM.

In order to emphasize the high variability of solar absorption in the extreme ultraviolet, Figure 11 shows the absorbed energy rate for five days between 1974 and 1979, i.e. from minimum (curve 1) to maximum (curve 5) solar activity conditions. Extreme ultraviolet irradiances (Torr et al. 1979) increase during that period, but composition and temperature in the neutral model are simultaneously modified. Furthermore, at 12 hours LST the solar zenith angle χ is not constant with seasons. As a result, there is no simple relation between the absorbed energy rate and the variations of solar extreme ultraviolet fluxes. Figure 11 indicates that around 150 km for the same local solar time, the absorbed energy rate can be much smaller for maximum solar activity than for minimum solar activity conditions. The vertical integral of the absorbed energy is, however, greater for maximum solar activity.

Since the first ionization potentials of O_2, O, N_2 and He are at 102.7 nm, 91.0 nm, 79.6 nm and 50.4 nm respectively, a significant part of the absorbed energy rate below 105 nm is consumed in ionization processes. Figures 12 and 13 show ion production rates at 12 hours LST on 18 july 1976 and 14 December 1978, respectively. These two days have been chosen since they correspond to the extreme solar zenith distances used previously. In Figure 12 the major ion production

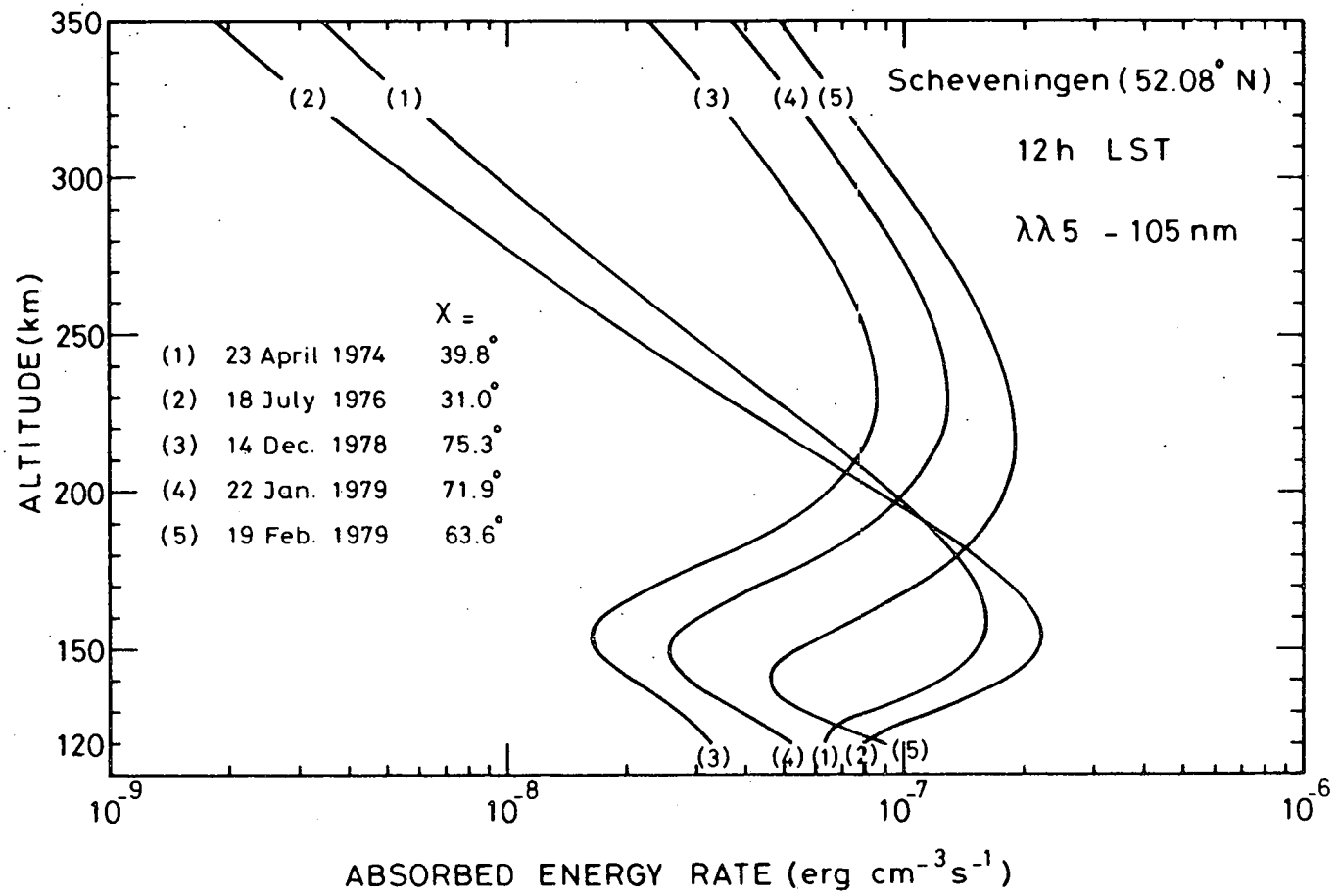

Fig. 11 : Absorbed energy rates above 120 km for the five days considered in Fig. 6. Solar zenith distances χ are given for each day.

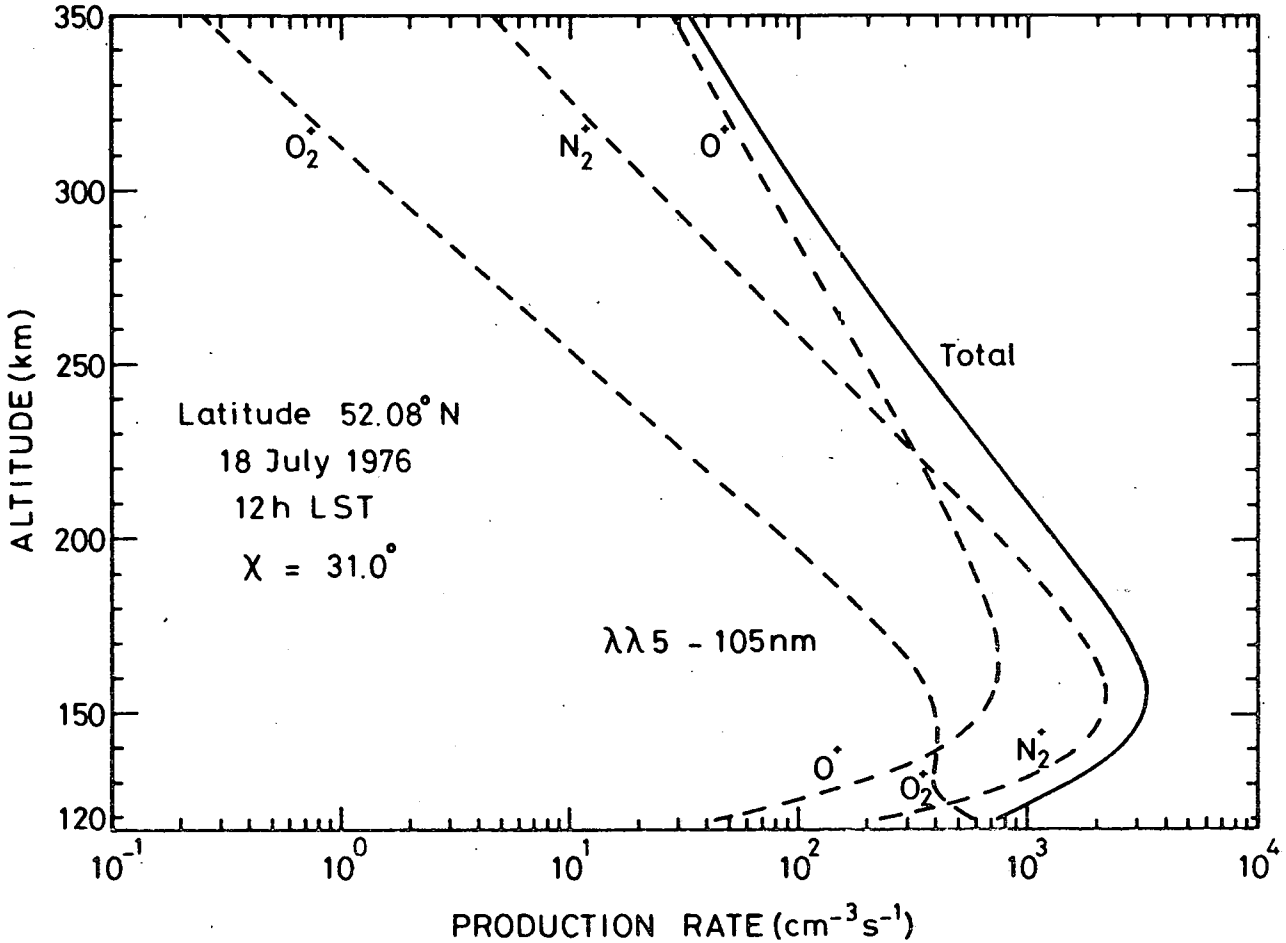

Fig. 12 : Total and partial ion production rates on 18 July 1976 at 12 hours LST in the extreme ultraviolet. Low solar activity conditions.

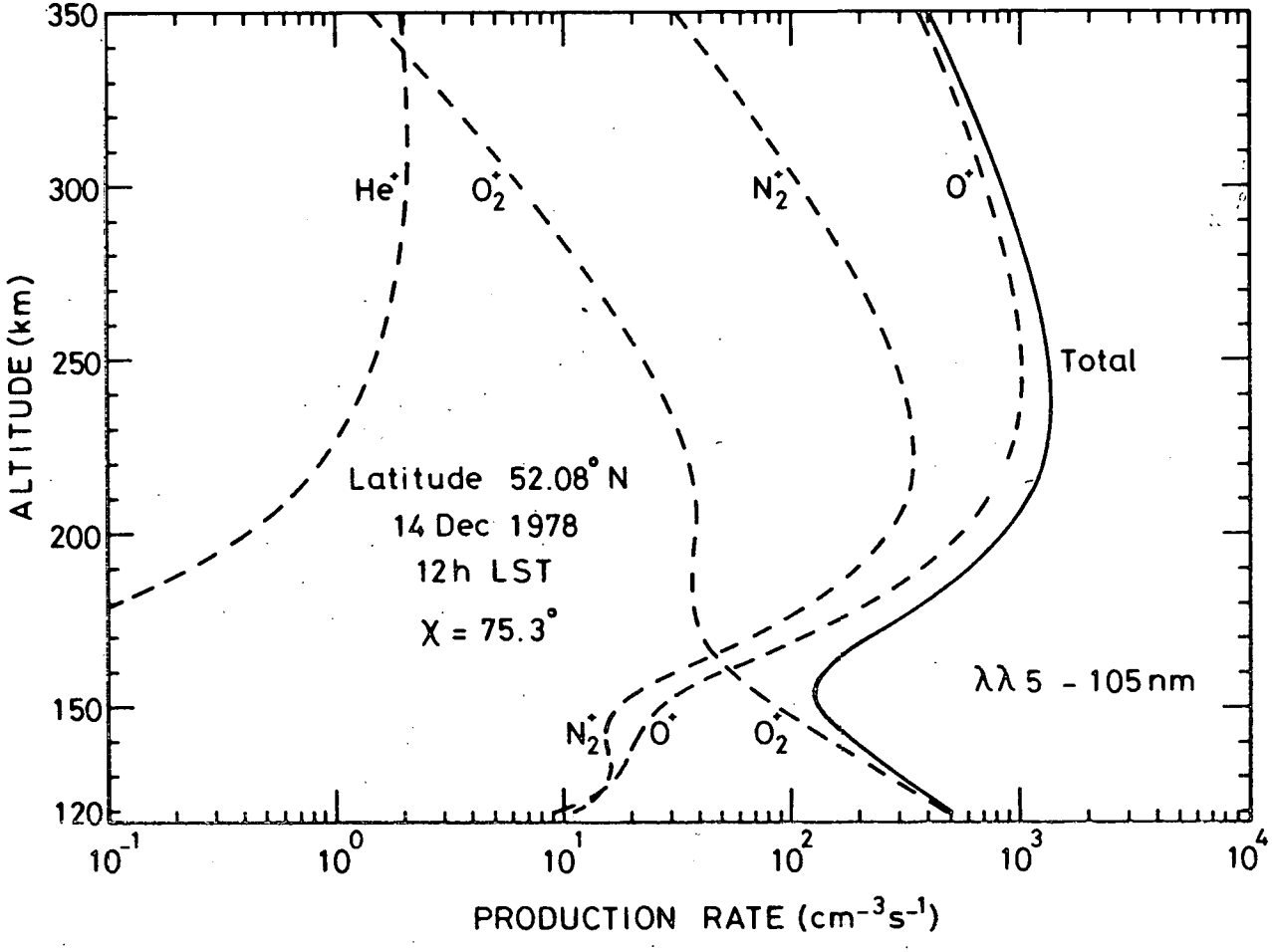

Fig. 13 : Same as Fig. 12 but for 14 December 1978. High solar activity conditions. He^+ ion production is apparent.

results from N_2 whereas the N_2^+ production rate is never the most important in Figure 13. Furthermore the He^+ production rate is completely negligible below 350 km in Figure 12. Actually the total ion production rates in Figures 12 and 13 follow closely the corresponding absorbed energy rates in Figure 11.

For a given extreme ultraviolet irradiance, ion production rates vary strongly during the day as it can be seen on Figures 14 and 15 where diurnal variations of N_2^+ and O^+ are shown at 150 km and 200 km altitude. Such an effect is a combination of the time variation of the solar zenith angle, and the diurnal variation of the neutral atmosphere. Both Figures indicate that ionic production is more important at 150 km than at 200 km for spring and summer conditions. During winter the opposite situation occurs and no simple dependence on solar activity can be deduced. Furthermore, a good knowledge of solar irradiances is required when specific applications are attempted. As an example, Taieb et al. (1978) explained an observed daytime valley in the ionospheric F_1 layer by introducing a downward ionization drift. These calculations were made by using Hinteregger's (1976) fluxes ($F_{10.7}$ = 73 x 10^{-22} Wm^{-2} Hz^{-1}) and measurements on board of AEROS-A (Schmidtke, 1976) when $F_{10.7}$ = 95 x 10^{-22} Wm^{-2} Hz^{-1}. Schmidtke's values were closer to the solar activity conditions at the time when the valley was observed and only these data lead to a good fit with the incoherent scatter results.

A fundamental parameter for the determination of the thermal structure of the upper atmosphere is the heating efficiency which is the fraction of the absorbed energy rate (see Figure 10) transfered into heat. Some of the absorbed energy is used for photodissociation, mainly in the Schumann-Runge continuum and below 102.6 nm some energy is consumed for ionization processes. The problem is, however, complicated by the fact that products of photodissociation such as excited atomic oxygen $O(^1D)$ can undergo collisional deactivation and can be transported a lower heights. Moreover, after the production of electron-

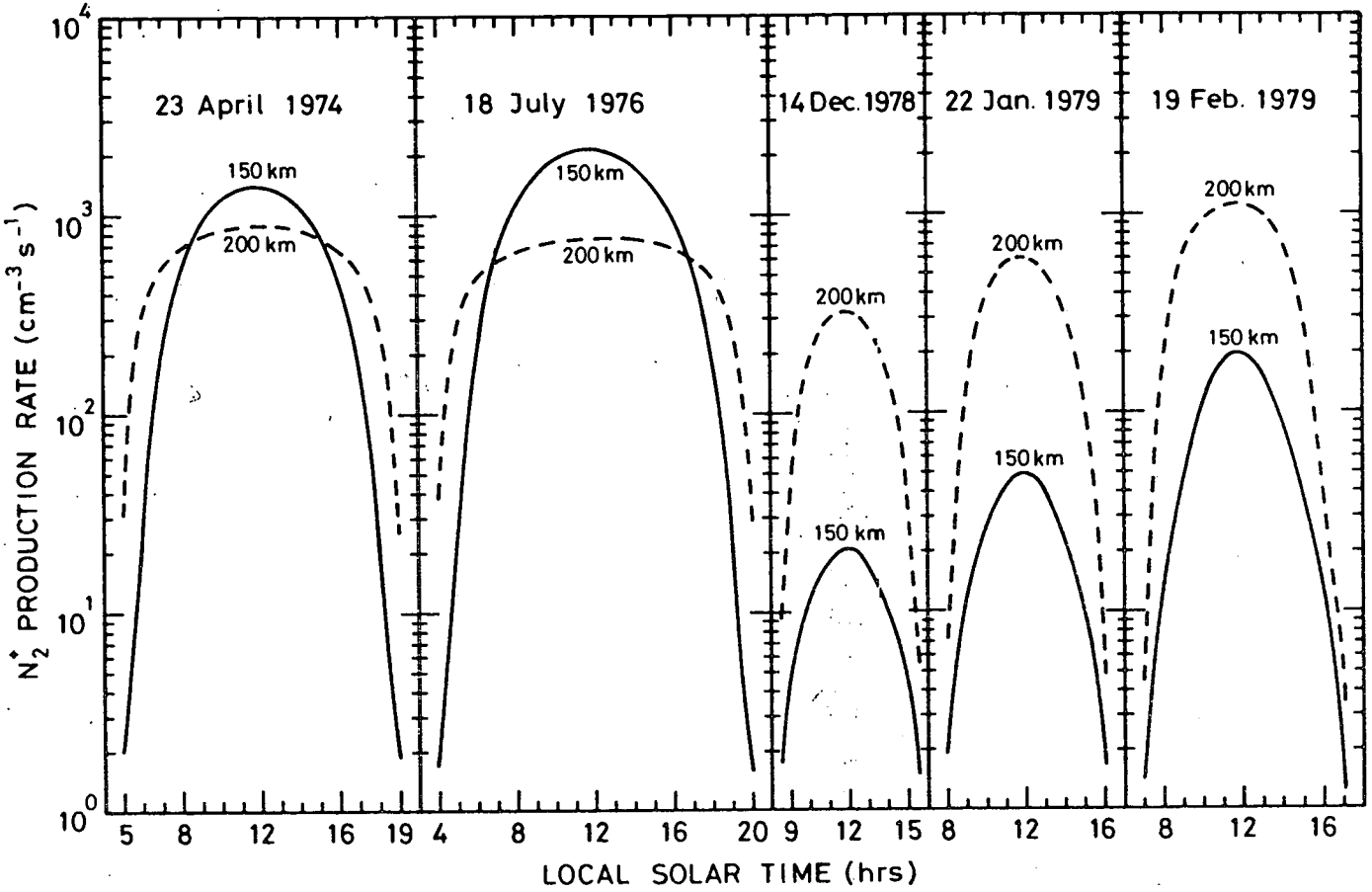

Fig. 14 : Daily variation of N_2^+ production rates at 150 km and 200 km. Solar activity increases from 1974 to 1979.

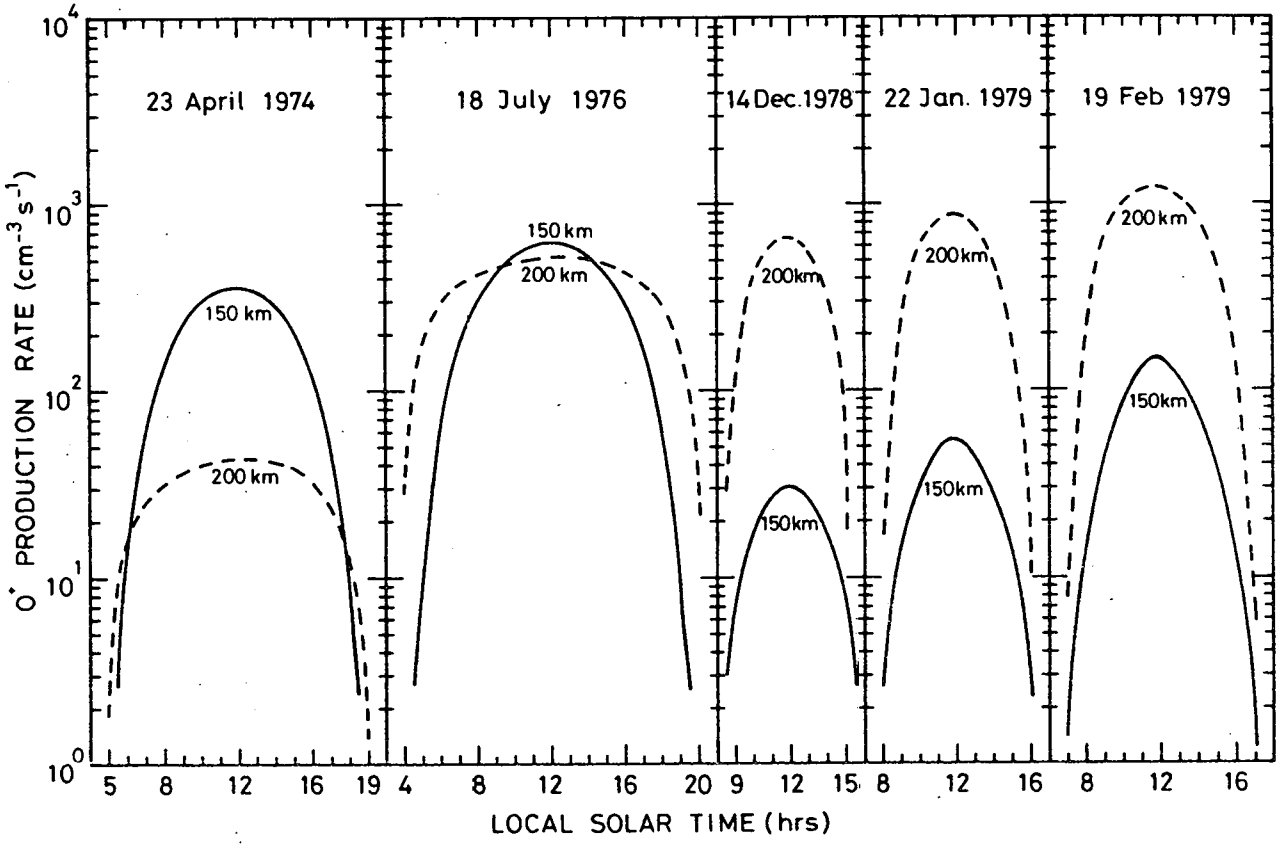

Fig. 15 : Daily variation of O^+ production rates for same conditions as in Fig. 14.

ion pairs the photoelectrons can excite neutral species leading to airglow phenomena and/or to atmospheric heating. Banks and Kockarts (1973b) suggested that the heating efficiency should depend on the solar cycle because the relative abundances of the different ions, atoms and molecules are variable. Recently, Torr et al. (1980) found that the heating efficiency is a function of altitude and solar cycle. It peaks actually near the height of maximum extreme ultraviolet absorption (see Figure 11) at a value of approximately 50%. At present time, it is extremely difficult to construct theoretical models which could give results comparable to those obtained in Figures 1a and 1b from semi-empirical models, since there are not enough solar ultraviolet irradiances available for all solar activity conditions. But, there are also high latitude heat sources which must be included in three-dimensional models. These high latitude heat sources result from particle precipitations and from Joule dissipation by electric currents (see Banks, 1977) and the whole thermosphere is influenced by dynamical interactions between the atmosphere, the ionosphere and the magnetosphere (see Mayr et al. 1978). High latitude heat sources may reach values as high as 100 erg cm^{-2} s^{-1} (Banks, 1977). But solar extreme ultraviolet is the most important heat source since it influences permanently 50% of the whole thermosphere.

Using the values of Torr et al. (1979) for the extreme ultraviolet, the values of Heroux and Hinteregger (1978) in the Schumann-Runge continuum and their variations quoted by Hinteregger (1981) and the Lyman-α variations of Vidal-Madjar (1975), the energetic variations of solar irradiances between minimum and maximum solar activity can be summarized as follows :

- from 5 nm to 105 nm, $E = (5 \pm 3)$ erg cm^{-2} s^{-1}
- from 105 nm to 175 nm, $E = (9 \pm 3)$ erg cm^{-2} s^{-1}
- at Lyman-α, $E = (6 \pm 2)$ erg cm^{-2} s^{-1}

When these irradiances are compared to the solar constant value of 1.367×10^6 erg cm^{-2} s^{-1} (Willson, 1978), it appears that observed variations in the solar ultraviolet fluxes only represent parts per million of the total electromagnetic emission of the Sun. It could seem surprising how such a small fraction can induce the observed large variations in the upper atmosphere. The quantitative importance of solar flux variations can be understood by comparing the total kinetic energy in a vertical atmospheric column to the solar energy which can be absorbed in such a column. Table I gives a rough comparison between these quantities. The available solar energy is estimated by assuming a 24 hours permanent illumination. It is, therefore, an upper limit. It is seen that the extreme ultraviolet energy (λλ 5-105 nm) is comparable to the kinetic energy present in a column above 100 km. Since this solar energy is actually absorbed in this column, it can strongly modify the thermospheric structure. The Schumann-Runge continuum including Lyman-α is comparable to the atmospheric kinetic energy down to the mesopause level. Even when the available solar energy is extended up to 200 nm or 300 nm it becomes less important compared to the existing kinetic energy in the stratosphere. As an example the energy available in the 5 nm-200 nm range represents only 1% of the kinetic energy at the stratopause. Between 200 nm and 300 nm absorption by ozone is clearly important in the stratosphere. But above 200 nm there is apparently not enough variation in the solar irradiance (Cook et al. 1980; Thuillier and Simon, 1981) to induce changes in the absorbed energy comparable to the atmospheric kinetic energy.

6. CONCLUSION

Some solar ultraviolet irradiances below 175 nm are now available for aeronomical applications. One solar cycle, however, can be very different from the next one (Hinteregger, 1979) and up to now no single measurement has ever been performed for very high solar activity such as in 1958. Considering the period from 1 January 1958 to 30 April 1980, i.e. 8156 days, it is possible to compute the probability

TABLE I : Kinetic energy column content and available solar energy for 24 hours illumination.

Altitude (km)	Kinetic energy (erg cm^{-2})	λλ(nm)	Solar energy (erg cm^{-2})
15	7.0×10^{10}	5-300	1.4×10^{9}
50	7.1×10^{8}	5-200	$(7 \pm 0.8) \times 10^{6}$
85	2.5×10^{6}	5-175	$(1.7 \pm 0.7) \times 10^{6}$
100	2.5×10^{5}	5-105	$(4.3 \pm 2.6) \times 10^{5}$

for finding solar activity conditions approximately identical to the decimetric fluxes F and $\bar{F}$ existing on the days when the five sets of irradiances used in this paper were measured. Figure 16 shows this probability as a function of simultaneous variations in the daily 10.7 cm flux and in the three solar rotation averaged values. Such a probability is seen to be very low, especially for high solar activity. In semi-empirical models a variation $\Delta F = \Delta\bar{F} = 10$ leads to a thermopause temperature variation of the order of 50 K and a quantitative determination of the variation of solar ultraviolet irradiances is far from being available for all solar activity conditions.

Independently of the complicated interaction between solar radiation and the Earth's atmosphere, it should be clear that solar irradiances constitute the most important upper boundary condition which should be determined with the highest possible accuracy. Since this upper boundary condition is changing over short and long time periods, many measurements are required before a definite picture of the variability can be established.

ACKNOWLEDGEMENTS

The programming help of E. Falise and the careful drawings of A. Simon were greatly appreciated.

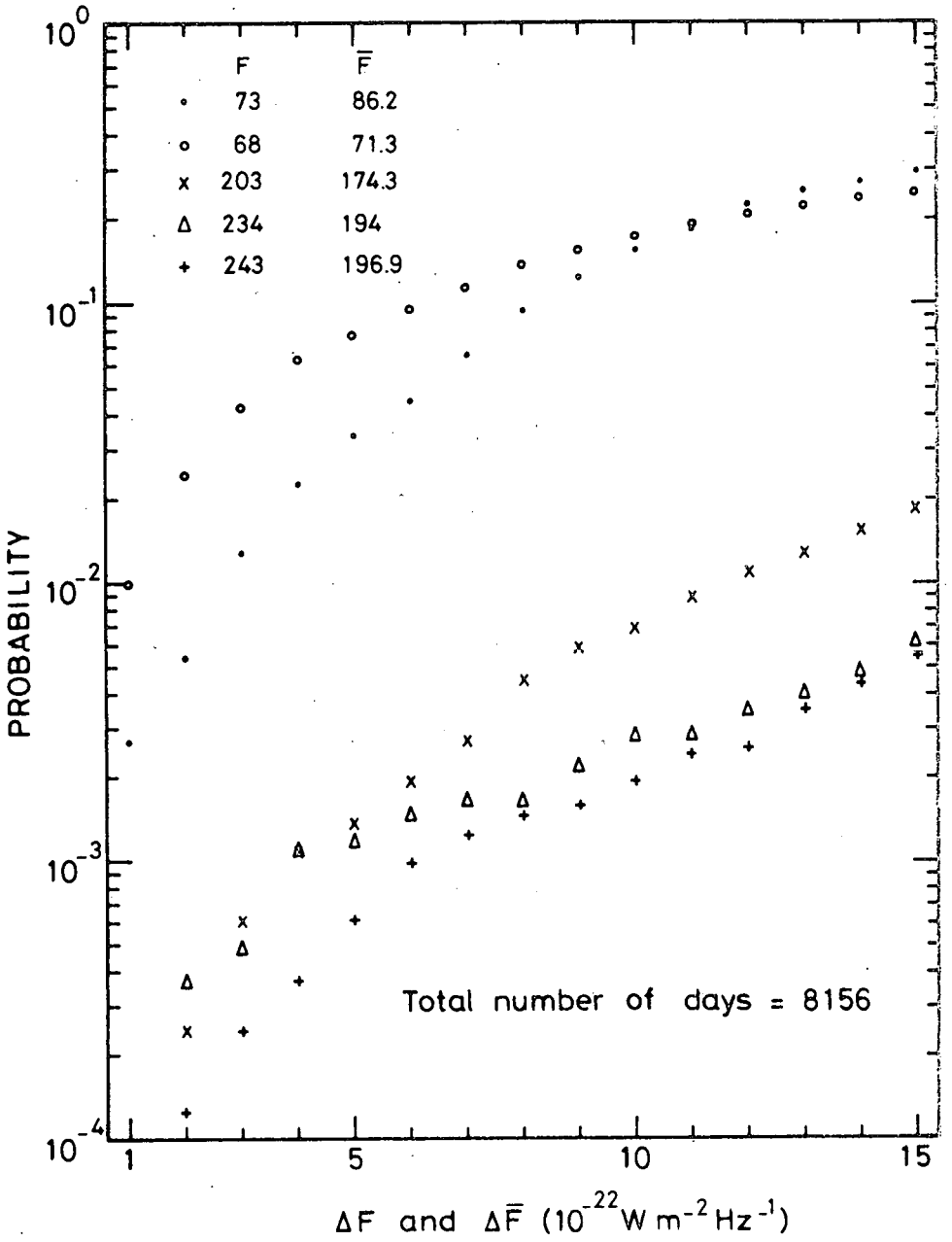

Fig. 16 : Probability to encounter solar flux conditions shown in the upper left corner as a function of simultaneous variations in the daily decimetric flux F and in the averaged values over three solar rotations. F = 73, on 23 April 1974; F = 68 on 18 July 1976; F = 203 on 14 December 1978; F = 234 on 22 January 1979; F = 243 on 19 February 1979. Probability of occurence has been computed over 8156 days extending from 1958 to 1980.

REFERENCES

Ackerman, M. : 1971, in G. Fiocco (ed.), Mesospheric Models and Related Experiments, D. Reidel Publ. Co., Dordrecht, Holland, p. 149.

Ackerman, M., Biaumé, F. and Kockarts, G. : 1970, Planet. Space Sci., 18, 1639.

Banks, P.M. : 1977, J. Atmos. Terr. Phys., 39, 179.

Banks, P.M. and Kockarts, G. : 1973a, Aeronomy Part A, Academic Press, New York.

Banks, P.M. and Kockarts, G. : 1973b, Aeronomy Part B, Academic Press, New York.

Barlier, F., Bauer, P., Jaeck, C., Thuillier, G. and Kockarts, G. : 1974, J. Geophys. Res., 79, 5273.

Barlier, F., Berger, C., Falin, J.L., Kockarts, G. and Thuillier, G. : 1978, Ann. Géophys., 34, 9.

Barlier, F., Berger, C., Falin, J.L., Kockarts, G. and Thuillier, G. : 1979, J. Atmos. Terr. Phys., 41, 527.

Bates, D.R. : 1959, Proc. Roy. Soc., 253, 451.

Bates, D.R. : 1973, J. Atmos. Terr. Phys. 35, 1935.

Bauer, P., Waldteufel, P. and Alcaydé, D. : 1970, J. Geophys. Res. 75, 4825.

Baum, W.A., Johnson, F.S., Oberly, J.J., Rockwood, C.C., Strain, C.W. and Tousey, R. : 1946, Phys. Rev. 70, 781.

Blamont, J.E. and Luton, J.M. : 1972, J. Geophys. Res. 77, 3534.

Carru, H., Petit, M. and Waldteufel, P. : 1967, Planet. Space Sci. 15, 944.

Champion, K.S.W. : 1967, Space Research 7, 1101.

Chapman, S. : 1931, Proc. Phys. Soc. 43, 483.

CIRA 1972 : Cospar International Reference Atmosphere, 450 pp., Akademie-Verlag, Berlin.

Cook, J.W., Brueckner, G.E. and Van Hoosier, M.E. : 1980, J. Geophys. Res. 85, 2257.

Groves, G.V. : 1959, Nature 184, 178.

Harris, I. and Priester, W. : 1962, J. Atmos. Sci. 19, 286.

Hedin, A.E., Mayr, H.G., Reber, C.A., Spencer, N.W. and Carignan, G.R. : 1974, J. Geophys. Res. 79, 215.

Hedin, A.E., Salah, J.E., Evans, J.V., Reber, C.A., Newton, G.P., Spencer, N.W., Kayser, D.C., Alcaydé, D., Bauer, P., Cogger, L. and McClure, J.P. : 1977a, J. Geophys. Res. 82, 2139.

Hedin, A.E., Reber, C.A., Newton, G.P., Spencer, N.W., Brinton, H.C. and Mayr, H.G. : 1977b, J. Geophys. Res. 82, 2148.

Heroux, L. and Hinteregger, H.A. : 1978, J. Geophys. Res. 83, 5305.

Hinteregger, H.E. : 1976, J. Atmos. Terr. Phys. 38, 791.

Hinteregger, H.E. : 1979, J. Geophys. Res. 84, 1933.

Hinteregger, H.E. : 1981, Adv. Space Res. 1 to be published.

Jacchia, L.G. : 1959, Nature 183, 526.

Jacchia, L.G. : 1965, Smith Contr. Astrophys. 8, 215.

Jacchia, L.G. : 1971, Smith Astrophys. Obs. Spec. Rep. 332.

Jacchia, L.G. : 1977, Smith. Astrophys. Obs. Spec. Rep. 375.

Jacchia, L.G. : 1979, Space Research 19, 179.

Johnson, F.S. : 1956, J. Geophys. Res. 61, 71.

Johnson, F.S., Purcell, J.D., Tousey, R. and Watanabe, K. : 1952, J. Geophys. Res. 57, 157.

Keating, G.M. and Prior, E.J. : 1968, Space Research 8, 982.

King-Hele, D.G. and Walker, D.M.C. : 1959, Nature 183, 527.

Kirby, K., Constantinides, E.R., Babeu, S., Oppenheimer, M. and Victor, G.A. : 1979, Atom. Data Nucl. Data Tables 23, 63.

Kockarts, G. : 1971, in G. Fiocco (ed.), Mesospheric Models and Related Experiments, D. Reidel Publ. Co., Dordrecht, Holland, p. 160.

Kockarts, G. : 1976, Planet. Space Sci. 24, 589.

Kockarts, G. : 1981, Adv. Space Res. 1, to be published.

Kockarts, G. and Nicolet, M. : 1962, Ann. Géophys. 18, 269.

Kockarts, G. and Nicolet, M. : 1963, Ann. Géophys. 19, 370.

Köhnlein, W. : 1980, Planet. Space Sci. 28, 225.

Lofthus, A. and Krupenie, P.H. : 1977, J. Phys. Chem. Ref. Data 6, 113.

Longmuire, M.S., Bartoe, J.-D.F., Brown, C.M., Brueckner, G.E. and Tousey, R. : 1979, J. Geophys. Res. 84, 1277.

Lowan, A.N. : 1955, J. Geophys. Res. 60, 421.

Mayr, H.G., Harris, I. and Spencer, N.W. : 1978, Rev. Geophys. Space Phys. 16, 539.

Mayr, H.G., Hedin, A.E., Reber, C.A. and Carignan, G.R. : 1974, J. Geophys. Res. 79, 619.

Milankovitch, M. : 1930, in Handbuch der Klimatologie, Band I, Teil A Mathematische Klimalehre, Verlag Borntraeger, Berlin.

Nisbet, J.S. : 1967, J. Atmos. Sci. 24, 586.

Ogawa, S. and Ogawa, M : 1975, Canad. J. Phys. 53, 1845.

Priester, W. : 1959, Naturwiss. 46, 197.

Ratcliffe, J.A. : 1978, Contemp. Phys. 6, 495.

Roemer, M. : 1971, Space Research 11, 965.

Salah, J.E., Evans, J.V., Alcaydé, D. and Bauer, P. : 1976, Ann. Géophys. 32, 257.

Samain, D. and Simon, P.C. : 1976, Solar Phys. 49, 33.

Schmidtke, G. : 1976, Geophys. Res. Letters 3, 573.

Swider, W. : 1964, Planet. Space Sci. 12, 761.

Swider, W. and Gardner, M.E. : 1969, Appl. Opt. 8, 725.

Taieb, C., Scialom, G. and Kockarts, G. : 1978, Planet. Space Sci. 26, 1007.

Thuillier, G., Falin, J.L. and Barlier, F. : 1977, J. Atmos. Terr. Phys. 39, 1195.

Thuillier, G. and Simon, P.C. : 1981, 14th ESLAB Symposium.

Torr, M.R., Torr, D.G., Ong, R.A. and Hinteregger, H.E. : 1979, Geophys. Res. Letters 6, 771.

Torr, M.R., Torr, D.G. and Richards, P.G. : 1980, Geophys. Res. Letters 7, 373.

Vidal-Madjar, A. : 1975, Solar Phys. 40, 69.

von Zahn, U., Köhnlein, W., Fricke, K.H., Laux, U., Trinks, H. and Volland, H. : 1977, Geophys. Res. Letters 4, 33.

Waynick, A.H. : 1975, Phil. Trans. R. Soc. Lond. A 280, 11.

Willson, R.C. : 1978, J. Geophys. Res. 83, 4003.